AD-A113 518 CHARLES STARK DRAPER LAB INC CAMBRIDGE MA F/G 13/9
MATERIALS RESEARCH FOR ADVANCED INERTIAL INSTRUMENTATION, TASK --ETC(U)
DEC 81 D DAS, K KUMAR, E WETTSTEIN, J WOLLAM N00014-77-C-0388
UNCLASSIFIED R-1528 NL

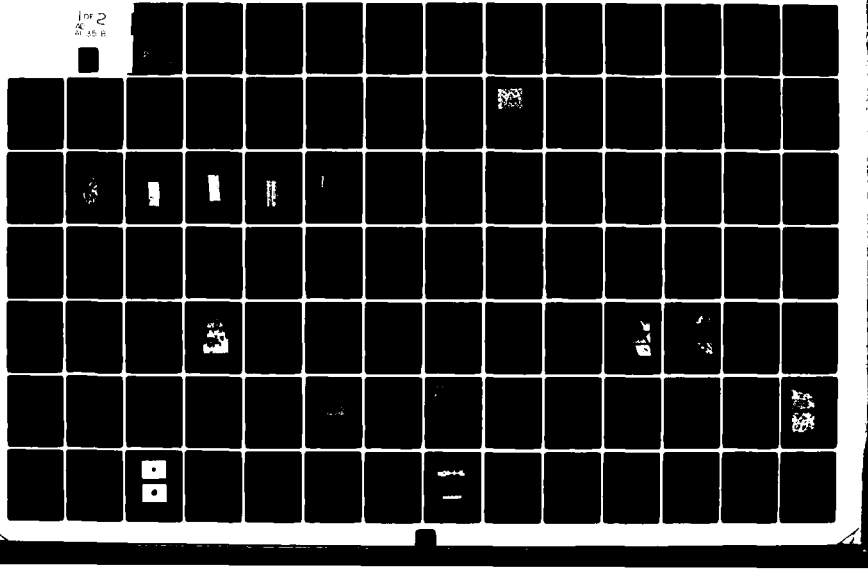

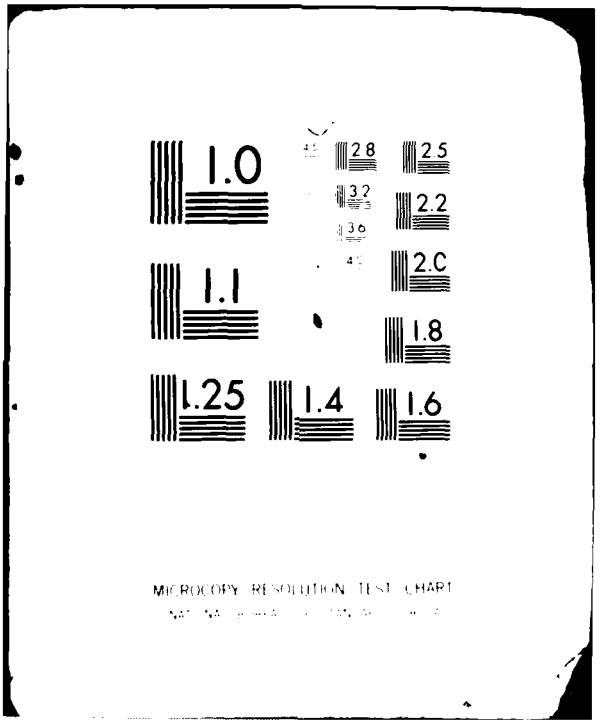
1.0
2.8
2.5
3.2
2.2
3.6
2.0
1.1
1.8
1.25
1.4
1.6
MICROCOPY RESOLUTION TEST CHART

AD A113518

(12)

R–1528

MATERIALS RESEARCH FOR ADVANCED INERTIAL INSTRUMENTATION

TASK 2: GAS BEARING MATERIAL DEVELOPMENT

DECEMBER 1981

TECHNICAL REPORT NO. 4
FOR THE PERIOD
1 OCTOBER 1980–30 SEPTEMBER 1981

BY

D. DAS, K. KUMAR, E. WETTSTEIN, J. WOLLAM

Prepared for the Office of Naval Research, Department of the Navy, under contract N00014-77-C-0388.

Approved for public release, distribution unlimited.

Permission is granted the U.S. Government to reproduce this paper in whole or in part.

The Charles Stark Draper Laboratory, Inc.
Cambridge, Massachusetts 02139

DTIC FILE COPY

DTIC
ELECTE
APR 13 1982
S
E

82 04 13 127

UNCLASSIFIED

SECURITY CLASSIFICATION OF THIS PAGE *(When Data Entered)*

REPORT DOCUMENTATION PAGE

READ INSTRUCTIONS BEFORE COMPLETING FORM

1. REPORT NUMBER: R-1528	2. GOVT ACCESSION NO.: AD-A113 578
3. RECIPIENT'S CATALOG NUMBER:	
4. TITLE *(and Subtitle)*: MATERIALS RESEARCH FOR ADVANCED INERTIAL INSTRUMENTATION; TASK 2: GAS BEARING MATERIAL DEVELOPMENT	5. TYPE OF REPORT & PERIOD COVERED: Research Report 10/1/80 - 9/30/81
	6. PERFORMING ORG. REPORT NUMBER: R-1528
7. AUTHOR(s): D. Das, K. Kumar, E. Wettstein, and J. Wollam	8. CONTRACT OR GRANT NUMBER(s): N00014-77-C-0388
9. PERFORMING ORGANIZATION NAME AND ADDRESS: The Charles Stark Draper Laboratory, Inc. 555 Technology Square Cambridge, Massachusetts 02139	10. PROGRAM ELEMENT, PROJECT, TASK AREA & WORK UNIT NUMBERS
11. CONTROLLING OFFICE NAME AND ADDRESS: Office of Naval Research Department of the Navy 800 N. Quincy St., Arlington, Virginia 20217	12. REPORT DATE: December 1981 13. NUMBER OF PAGES: 102
14. MONITORING AGENCY NAME & ADDRESS *(if different from Controlling Office)*: Office of Naval Research Boston Branch, Bldg. 114, Sec. D 666 Summer Street Boston, Massachusetts 02210	15. SECURITY CLASS. *(of this report)*: Unclassified 15a. DECLASSIFICATION/DOWNGRADING SCHEDULE

16. DISTRIBUTION STATEMENT *(of this Report)*

Approved for public release; distribution unlimited.

17. DISTRIBUTION STATEMENT *(of the abstract entered in Block 20, if different from Report)*

18. SUPPLEMENTARY NOTES

19. KEY WORDS *(Continue on reverse side if necessary and identify by block number)*

Beryllium	Boron	Beryllium-Ceramin Composite
Ion implantation	Reactive Diffusion	Hot Isostatic Pressing (HIP)
CVD	Metal Matrix Composite	

20. ABSTRACT *(Continue on reverse side if necessary and identify by block number)*

The gas bearing materials development program includes three approaches: (1) chemical vapor deposition and subsequent reactive diffusion of boron on beryllium, (2) ion implantation of boron into beryllium, and (3) development of a beryllium-ceramic composite material.

(1) The chemical vapor deposition (CVD) process at (higher) temperatures of 850° to 950°C produced thin, hard, multiphase coatings compared (continued)

DD FORM 1 JAN 73 1473 EDITION OF 1 NOV 65 IS OBSOLETE

UNCLASSIFIED

SECURITY CLASSIFICATION OF THIS PAGE *(When Data Entered)*

to thicker coatings of boron at lower temperatures of 700° to 800°C. No deterioration of quality was observed upon increasing the sample size. (Larger samples were needed for wear and friction measurements using pin-on-disc testing, with sapphire balls serving as pins.) Friction coefficients were found to be about half those of beryllium and the wear tracks were smooth with no sign of plowing or pullouts. CVD film thicknesses were found to be non-uniform and were attributed to convection currents in the CVD gas around the hot beryllium sample. A correction of the situation is being sought by rotating the sample during CVD.

(2) Conventionally machined, and subsequently stress-relieved, beryllium discs were polished and implanted with boron, some at a local facility and others at the Naval Research Laboratory (NRL). A variety of implants were attempted. Included among these were flat, graded and single-dose composition profiles. The locally produced samples appeared severely oxidized, unlike the NRL samples which were quite satisfactory. Subsequent analyses using Rutherford Back Scattering (RBS) and Auger Electron Microscopy (AES) showed that whereas the desired profiles were obtained on the NRL materials the same was not true of the local samples. (A reasonably good correlation was noted for the RBS and AES data.) Wear testing was, therefore, mainly confined to the NRL samples. A flex-pivot wear tester capable of both pin-on-disc and disc-on-disc testing was developed for this purpose. Experiments showed that for an identical surface concentration a flat boron profile was substantially superior in terms of resisting wear, compared to a graded boron distribution. This indicated that the wear mechanism was strongly influenced by what existed in the subsurface regions in addition to the conditions in the immediate region of contact. Differences were observed for the friction traces of the implanted specimens with respect to beryllium. A most notable feature was the existence of three distinct regions in the implanted materials, and these were attributed to effects resulting from gradual wearing off of the implanted layer.

(3) Additional lapping studies were performed during this reporting period on the Be-TiB_2 materials with fine diamond particles as the abrasive medium. The use of diamond resulted in damage (observed primarily as pits) in the TiB_2 particles dispersed in the composite. Further lapping of the samples with fine-particle Al_2O_3 and Syton (which is a suspension of ultra-fine SiO_2 particles) removed much of this damage. Considerable relief of the ceramic particles, however, resulted from these latter procedures, with more ceramic particle relief observed for Al_2O_3 than for Syton. Techniques continue to be investigated and developed for suitable wear testing of these composites. In experiments performed thus far, material accretion (from wear of the pin) rather than depletion (from wear of the sample) has been observed. Thermal expansion data were collected on different Be-TiB_2 powders as well as towards eventual near-net shape fabrication of desired gas bearing parts. Industrial application of these materials is currently being investigated. Experiments performed to date show excellent promise.

R-1528

MATERIALS RESEARCH FOR ADVANCED INERTIAL INSTRUMENTATION

TASK 2: GAS BEARING MATERIAL DEVELOPMENT

DECEMBER 1981

TECHNICAL REPORT NO. 4

FOR THE PERIOD

1 October 1980 - 30 September 1981

D. Das, K. Kumar, E. Wettstein, J. Wollam

Prepared for the Office of Naval Research,
Department of the Navy, under Contract N00014-77-C-0388.

Approved for public release; distribution unlimited.

Permission is granted to the U.S. Government
to reproduce this report in whole or in part.

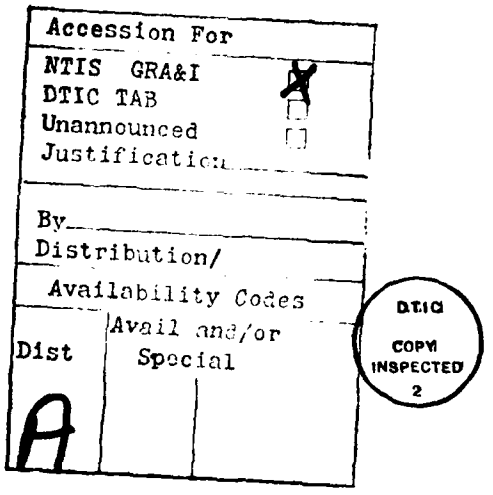

Approved:

M.S. Sapuppo, Head
Component Development Department

The Charles Stark Draper Laboratory, Inc.
Cambridge, Massachusetts 02139

ACKNOWLEDGEMENT

This report was prepared by The Charles Stark Draper Laboratory, Inc. under Contract N00014-77-C-0388 with the Office of Naval Research of the Department of the Navy.

Publication of this report does not constitute approval by the U.S. Navy of the findings or conclusions contained herein. It is published for the exchange and stimulation of ideas.

TABLE OF CONTENTS (Continued)

TABLE OF CONTENTS

LIST OF FIGURES

LIST OF FIGURES (Continued)

LIST OF TABLES

SECTION 1

INTRODUCTION

The material of choice in the fabrication of structural members for state-of-the-art inertial instruments is beryllium primarily because of properties such as high values of stiffness, thermal conductivity, and the strength-to-density ratio that it possesses. Unfortunately, gas bearings used in such instruments require substantially greater hardness and wear resistance at the mating surfaces than beryllium offers.

Gas bearings initially built at The Charles Stark Draper Laboratory, Inc., (CSDL) involved fabricating entire bearings out of solid pieces of ceramic. These ceramics were typically produced by sintering and hot pressing techniques. Difficulties were encountered in machining these materials, making the process expensive and time consuming. An additional disadvantage in the use of ceramics for this purpose was the physical incompatibility of the resultant gas bearings with the other structural members of the gyro. (Differences in thermal expansion characteristics and low values of thermal conductivity of these materials result in undesirable strains and temperature variations in the assembly. This leads to a variety of instrument instabilities which adversely affect the accuracy and reliability of the several inertial components.) The high cost in money and time, in addition to the problems stemming from low values of thermal expansion and thermal conductivity for ceramics, caused this option to be discarded.

The subsequent rationale developed to resolve the discrepancies envisioned the use of two different materials, since no single material was known to meet all demands. One material (beryllium) was to form the structural member and satisfy bulk property requirements and the other was to be deposited as a coating to yield a low-friction, wear-resistant surface for the gas bearing. Operational and processing problems have,

nevertheless, persisted even with the approaches that resulted from this rationale and a better materials system is needed. The present task addresses this latter requirement through research efforts on new materials and processes for gyroscopes with gas bearings.

SECTION 2

PRESENT WORK

2.1 Limitations of Present Technology

The property requirements of the coatings formed on gas bearing surfaces are summarized as follows:

(1) High resistance to wear from sliding, erosion, and impact, for extended bearing life and stable performance.

(2) Low coefficient of friction for minimum starting torque.

(3) Zero surface porosity, for maximum gas bearing stiffness and minimum contamination entrapment.

These property requirements necessitate the selection of ceramic-type compositions for coating fabrication. Two methods of applying such coatings that have received attention in this area are plasma-spraying and sputtering, the former enjoying the wider use in production. With plasma spraying it is easy to apply coatings which are several thousandths of an inch thick, while the thicknesses of sputtered films are generally less than that by about two orders of magnitude. Examples of the use of these processes are the plasma-sprayed chromium oxide and aluminum oxide coatings now in use in several instrument designs and the sputter-deposited tungsten carbide and titanium carbide coatings that have been subjects of some past development activity.

The one feature common to both sprayed and sputtered coatings is the difference in physical properties between the coating and the substrate. While this may be somewhat tolerable in thin films produced by sputtering, thicker films made by spraying are susceptible to failure from the imperfect match of expansion coefficients at the coating-

substrate interface. To reduce stresses that result from differences in expansion coefficients, spraying is generally conducted at lower spray temperatures. However, this adversely affects interparticle cohesive strength, which results in pull-outs during polishing and lapping operations, and generation of wear debris in active service. The clearance between the mating parts of a gas bearing is only about 50 microinches so that even the mildest form of wear (mildest by conventional standards) can prove to be catastrophic in gas bearing applications.

A more severe problem that has been found in sprayed deposits is the presence of interconnecting porous structures in the coating. The effect of this interconnected porosity is to provide a shunt path for gas flow such that the hydrodynamic pressure rise is attenuated from that attainable with a nonporous coating.[1]* This, in turn, causes a lower load capacity and stiffness for the gas bearing. In addition to this most severe effect, the porosity at the surface also results in effectively increasing the bearing gap beyond the physical (design) clearance.

The adhesion of the coating to the substrate is an important consideration in wear performance. The forces that give rise to adhesion in films made from both these proceses can be both mechanical and chemical in nature. The adhesion observed for deposits fabricated using the arc-plasma technology is generally found to be influenced by mechanical interlocking of the film on the external features of a substrate.

In chemically-compatible coating-substrate systems, the adhesion strength can be increased by depositing films at elevated temperatures. Elevated temperature deposition is therefore perferable to post-deposition heat treatment since ceramic materials generally behave well under mild compressive loading.

*Superscripted numerals refer to sources in the List of References.

Poor adhesion has been the biggest problem with sputtered ceramic coatings formed on beryllium substrates.[2] Sputter deposited films have also shown large deviations from stoichiometric composition and the presence of undesirable microstructures.

2.2 Direction of the Present Work

The broad objective which underlies all aspects of the present effort is to establish a hard, pore-free, wear-resistant surface which is integral with the beryllium structural members, thus eliminating the adhesion problems that have been encountered in the past. In the case-hardening subtask, this is approached by treating a beryllium surface with boron, with which it forms hard compounds. Boron enrichment of the surface, in one process, is accomplished by reactive diffusion of a freshly formed film of boron with the underlying beryllium. In another part of the work, boron ions are forced by an electrical potential to penetrate into the beryllium surface by ion implantation, a process which is relatively immune to native oxide barriers, solubilities, and diffusion coefficients.

In a second subtask the desired hardening and wear resistance are imparted by particles of a hard ceramic phase dispersed within the beryllium matrix. Such a metal-matrix composite is produced using powder metallurgy methods.

SECTION 3

Be-B REACTIVE DIFFUSION

3.1 Background

The approach taken in this part of the gas bearing materials development program was to produce a metallurgically bonded coating of boride or borides of beryllium formed by reactive diffusion of boron on the beryllium surface. The binary alloy system Be-B, according to published literature, contains four intermetallic compounds, Be_4B, Be_2B, BeB_2 and BeB_6. The two boron-rich compounds BeB_2 and BeB_6 are reported to have hardness values of 3200 and 2600 KHN respectively.[3,4,5] Boron also has a high hardness value of 3000 KHN. Reactive diffusion of boron on beryllium is therefore an attractive means of producing a metallurgically bonded hard surface coating.

3.2 Progress Prior to This Reporting Period

3.2.1 Chemical Vapor Deposition (CVD)

Of the two gaseous CVD systems, (1) chemical reaction of BCl_3 with H_2[6] and (2) thermal decomposition of diborane (B_2H_6),[7] the first one was found to be satisfactory at temperatures of 900°C and higher. At lower temperatures of operation, which are more desirable for beryllium substrates, B_2H_6 turned out to be the superior system. Initial experiments were performed inside a 1-1/4-inch-diameter quartz tube evacuable to 10 millitorr pressure prior to the introduction of the CVD gas. The samples were heated by RF induction with a coil wrapped around the quartz tube where the sample was located. At CVD temperatures of 850 to 900°C, coatings with a maximum thickness of 1 μm were formed with rusty pink color and maximum microhardness values of about 1200 KHN. Up to 5 μm thick steel gray color coatings with microhardness values exceeding 2000 KHN were subsequently formed at CVD

temperatures of 700 to 800°C. At this point it became apparent that thicker coatings of higher microhardness values would require a cleaner CVD system.

A new CVD system was built, consisting of a stainless steel bell jar equipped with high vacuum pumping systems and all stainless steel plumbing. The system was capable of being baked out and achieving a high vacuum of about 10^{-7} torr. A 20-kw RF generator was acquired for furnishing the induction heating power to the coil located inside the bell jar, which permitted increasing the sample size from 1/2-inch diameter discs to much larger sample sizes by the use of larger coils. Present capability is therefore adequate for producing CVD coating on actual gas bearing components. Initial experiments in this new system were carried out on 1/2-inch diameter samples using a 3/4-inch ID RF coil. The CVD procedure involved evacuating and baking out of the system at a low temperature of 100°C, following which the CVD was carried out using diborane gas (99.9% A + 0.1% B_2H_6) at atmospheric pressure. During the CVD run the bell jar was watercooled to prevent evolution of undesirable gases from the CVD chamber walls. Well bonded coatings up to 10 μm thick with uniform coverage of the entire 1/2-inch diameter surface were obtained at 700 and 800°C.[8] Microhardness values exceeded 3000 KHN measured under 25 gram indentation load. The low temperature CVD samples prepared in the older CVD apparatus had hardness values of around 1000 KHN at 25 gm load although at 5 to 10 gm load the measured values were above 2000 KHN. The quality had therefore improved substantially.

Metallography, electron diffraction and Auger analysis of these latest samples suggested that the CVD coatings consisted of an amorphous outer layer of boron with a layer of mixed beryllium borides at the interface. Heat treatment of the sample at 900°C for several hours converted the outer surface to BeB_6. More rigorous heat treatment was expected to produce BeB_2.

3.2.2 Study of Diffusion Kinetics in the Be-B System

A knowledge of the diffusion kinetics in the Be-B system was deemed necessary for both an understanding of the mechanism of formation of a boride coating on a beryllium surface by reactive diffusion as well as for precise coating control to produce an optimum wear surface. Early attempts at producing diffusion couples of the two elements by the conventional hot pressing technique failed because of the formation of a barrier layer of BeO on the beryllium surface.

To avoid the above problems, diffusion couples of Be-B were prepared by the hot isostatic pressing (HIP) technique. Solid pieces of the high temperature form of boron (β), available commercially, and the low temperature form of boron (γ) produced by the arc-plasma spray process at Draper Laboratory[9] were buried in beryllium powder and compacted. The compacts were then HIPed, which produced well-bonded interfaces between the boron pieces and the near theoretical density beryllium. The diffusion couples were removed from the HIPed compact by careful machining. Diffusion heat treatments, however, produced unexpected failures caused by the separation of the beryllium from the diffusion zone.

In spite of the failure of the diffusion couples to generate diffusion data, there was one other possibility of generating some information from the heat treatment of CVD processed samples. BeB_6 was formed on the surface of a CVD coated sample by heat treatment which was 100 percent amorphous boron initially. Based on this finding, it appeared that some meaningful diffusion data might evolve from heat treatments and analysis of the coating chemistry and structure.

3.3 Progress During the Reporting Period

The experimental investigations were carried on in the following areas:

(1) Higher temperature deposition

(2) Increased size of sample

(3) Preliminary wear and friction tests

(4) Diffusion anneal

(5) Preparation of pure Be-boride compounds

3.3.1 Deposition at 850 and 900°C

In the earlier CVD apparatus, the coatings produced between 850 and 950°C could not be made any thicker than about 1 μm with maximum measured microhardness values of 1200 KHN. Temperatures of 700 and 800°C allowed thicknesses to be built up to about 5 μm with the microhardness values exceeding 2000 KHN. Using the new CVD apparatus, film thicknesses of 10 μm could be easily produced at the lower temperatuares with microhardness values of over 3000 KHN. Therefore a number of deposition runs were made at 850°C and 900°C for times of 30 minutes to 2 hours. Gas flow was maintained at 1 liter/minute, which was the same as was used in the lower temperature depositions. The coatings in all cases were found to be spalling off at the edges. The two best coatings corresponded to sample No. 29 CVDed at 850°C for 2 hours and sample No. 30 at 900°C for 1 hour.

The above two samples were given a mild polish with 1 micron alumina-water slurry prior to hardness measurements. Since the CVD is performed on metallographically polished samples, the very mild polishing is adequate to produce a metallographic polish on the deposited surface, with a minimal removal of the coating. This final polishing serves a dual purpose of making the hardness indentations clearly defined and the microstructures, if present, readily observed. In the case of 700 and 800°C coatings the only feature observed in the microstructure was a polished metallic gray surface.

The 850° and 900°C samples however, showed multiphase structures with pink, blue-gray and white colors. Figures 1 and 2 are black and white microphotographs of the structures seen on the polished surface of the two samples CVDed at 850°C for 2 hours and 900°C for 1 hour respectively. Both of these samples show three distinct colors indicating the presence of three different phases.

In a binary system such as Be-B, the presence of three separate phases is an indication of a non-equilibrium condition. There are some beryllium borides which will match the colors seen. However, at this time the phases remain unknown and call for analytical procedures that may identify these phases. In Section 3.3.5 discussions will be given on the procedures to be used for these identifications.

Before going into a discussion of microhardness measurements, the orientation of the sample during the CVD operation should be explained. The sample is supported on wire pins, fitted into two small holes drilled on the edge of the sample, which keep the surface to be coated in a vertical plane inside the horizontal RF coil facing an open end of the coil. This plane is perpendicular to the direction of the CVD gas flow in a horizontal direction through a nozzle. Therefore the CVD surface nearest to the support holes will be referred to as the bottom part of the sample, and the diametrically opposite edge will be designated as the top part of the sample. Microhardness measurements were performed on samples 29 and 30 and the data are shown in Table 1.

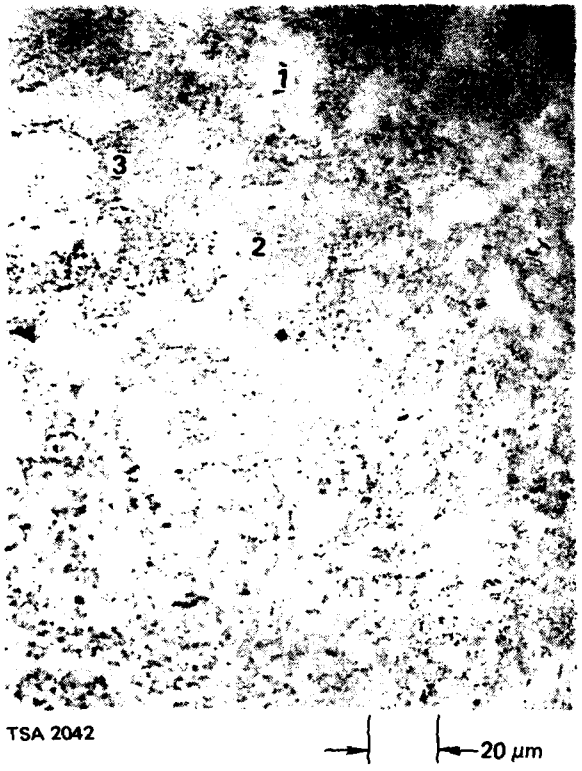

Figure 1. As polished microstructure of B-CVDed Be surface at 850°C for 2 hours. (1) Light gray matrix, (2) blue-gray grains and (3) pink and light entectic type structure.

Figure 2. As polished microstructure of B-CVDed Be surface at 900°C for 1 hour. (1) Smooth light matrix, (2) large blue-gray grains and (3) smaller pink grains.

Table 1. Microhardness of samples CVDed at 850°C and 900°C.

Area of Sample	Indentation Load (gms)	Microhardness Values at Various Loads (KHN)			
		Sample #29 - 850°C, 2 hrs		Sample #30 - 900°C, 1 hr	
		Average	Highest	Average	Highest
Top	50	145	176	398	486
Top	25	281	390	1160	1510
Top	10	435	638	2985	3380
Top	5	1200	2040		
Top	2	1586	3070		
Middle	50	142	174	568	719
Middle	25	297	317	1796	2250
Middle	10	841	1310	4104	4390
Middle	5	2463	4160		
Middle	2	2035	2550		
Bottom	50	180	273	1149	1440
Bottom	25			1793	2400
Bottom	10	2456	2690	3235	3840
Bottom	5	2020	2940		
Bottom	2	3450	4350		

Each of the hardness values shown in Table 1 is an average of 3 to 5 indentations placed in close proximity. In some cases there were large variations between the individual hardness values. However, the average hardness values follow the expected higher values at lower indentation loads. Similar behavior of the peak values are also evident. The only exception to the above behavior is seen in the case of hardness values for the middle part of sample No. 29 at 5 gm load for both the average and peak values which are larger than the values obtained with the indentation load of 2 gm.

At the first glance at Table 1, it would appear that the 900°C - 1-hour CVD resulted in higher values of microhardness than the 850°C - 2-hour CVD. But a more careful study shows that the inherent hardness values are the same in both cases. The only differences are that the higher values of hardness that are seen on sample No. 30 also show up in sample No. 29 at lower indentation load.

A conclusion might be drawn that the 900°C - 1 hr film is thicker. This, however, is contrary to our previous findings that lower temperatures produced heavier films. It would be better to defer any of the above conclusions until further studies of these samples with respect to their chemistry and microstructure have been planned.

A fact that should be noted is that the highest microhardness values in these samples are in the neighborhood of 3000 KHN, which is a substantial improvement over the maximum hardness values of about 1200 KHN seen in the samples at comparable temperatures in the earlier apparatus.

A disturbing fact about the deposition process is the non-uniformity of the coating. The top parts of the films are thinner than the bottom parts. This effect became more pronounced as experiments were carried out later with larger samples. It is believed to be associated with the flow characteristic of the CVD gas around the heated specimen. Plans have been formulated to rotate the specimen about its axis using a bellows type rotating mechanism inside the chamber and a motorized drive located outside the chamber.

3.3.2 Increased Size of Sample

Until March of 1981, the CVD experiments were performed on 1/2-inch diameter specimens using a 3/4-inch ID RF coil. At this time it was decided to perform such experiments on larger samples to determine if the quality of the coatings would be as good as they had been on smaller samples. Another reason for the change-over to larger specimen preparation was that the wear and friction measurement apparatus that was being built would require a minimum specimen size of 3/4-inch diameter discs. Consequently, the 3/4-inch ID RF coil was replaced with a 1-1/4-inch ID RF coil. The impedance of the RF generator was adjusted for a maximum output in the new coil. Preliminary heating tests performed with a 3/4-inch stainless steel disc indicated that similar size beryllium discs would easily be heated to deposition temperatures.

A few CVD runs were made at 700 and 800°C using 3/4-inch beryllium discs. The initial deposits were sooty and non-adherent. The system was then thoroughly checked for leaks and a number of leaks were found and corrected. In the process of checking, some oil contamination was discovered on the CVD chamber wall. The oil was cleaned off and the system was given a good bake out. With the system completely cleaned out and all leaks eliminated, the CVD film quality improved. Once again, the coatings began to show soundness with excellent adherence to the beryllium substrate.

3.3.3 Wear and Friction Measurements

Some preliminary wear and friction tests have now been performed on CVD boron films on beryllium. Since the highest microhardness values were obtained on surfaces prepared at 700°C, the coatings for initial wear and friction tests were CVDed on the samples at 700°C for 1/2 hour, 1 hour and 2 hours. The samples were given a light final polish with 0.1 μm Al_2O_3 and the microhardness values measured. The hardness values are shown in Table 2.

Table 2. Microhardness values of 700°C CVD samples for wear testing.

Sample #	Time (hrs) at CVD - 700°C	Microhardness at 25 gm Load	
		Top	Bottom
40	1	2400 KHN	3150 KHN
41	2	3150 KHN	4980 KHN
42	0.5	1370 KHN	1735 KHN

All of the samples listed in Table 2 appeared to be sound with no chipping. Hardness values increased monotonically with the duration of CVD. The bottom parts of each sample had thicker films than the top portions as indicated by their hardness values. But even the lowest value of 1370 KHN, under 25-gm load observed on the 1/2-hour CVD sample on the thinly coated region, was presumed to be high enough to render it fairly resistant to wear.

The above three samples following the hardness measurements were tested in the wear and friction testing apparatus that has been built recently at Draper Laboratory[10] for use with prototype gas bearing materials. The tester would accommodate either pin-on-disc or disc-on-disc testing. The apparatus that was built is briefly described in Section 4 of this report.

The testing mode selected for the present samples was the pin-on-disc type. The termination of the pin was a rigidly held 1/8-inch sapphire ball. The load on the stationary pin was 30 gm, resting on the rotating sample about 0.25 inch from the center of rotation. Samples were rotated at 200 r/min for 5 minutes and the circular wear tracks were approximately 1/2 inch in diameter. This amounted to a speed of the pin on the surface of 398 cm/min. The rotation of the test disc required a restraining torque on the pin to maintain its position. This restraining torque is a direct measure of the dynamic friction coefficient between the pin and the disc and is given by

$$T = \mu PR \qquad (1)$$

where

T is the torque
P is the normal load
R is the radius of the wear track
μ is the friction coefficient

The output E_o (in mV) from the signal generator is proportional to the torque:

$$E_o = S_{SG}T$$

where

S_{SG} is the signal generator sensitivity (calibrated at 120 mV/in-oz for the CSDL apparatus)

Therefore

$$\mu = \frac{E_o}{S_{SG}} \times \frac{1}{PR} \quad (P \text{ in oz, } R \text{ in in}) \qquad (2)$$

Aside from the evaluation of the coated samples, friction and wear measurements were also performed on a polished beryllium disc, similar to the ones that were CVD coated with boron. The measured signal E_o and the calculated friction values for the samples are shown in Table 3. The calculations were based on equation 2, using S_{SG} = 120 mV/in-oz, P = 30 gm = 1.06 oz and R = 0.25 inch.

Table 3. The E_o and μ values of CVD samples and uncoated Be disc.

Sample	At the Beginning		At the End	
	E_o(mV)	μ	E_o(mV)	μ
40	9	0.28	12	0.38
41	13	0.41	13	0.41
42	5	0.16	13	0.41
Uncoated Be	22	0.70	22	0.70

Various trial runs were then made on beryllium surfaces to determine the speed and load conditions under which the CSDL wear tester would produce reproducible and accurate friction coefficient values. It was determined that reduced linear speed of the sapphire ball at even higher loads than used in our preliminary runs gave more reproducible results. Based on these new findings three more wear test runs were made on the uncoated beryllium specimen in closely spaced concentric circles at a rotational speed of 100 r/min for 10 minutes under a load of 50 gm on the pin. The results of these new runs are shown in Table 4.

Table 4. Wear and friction tests on the uncoated beryllium sample.

Run #	r/min.	Load (gm)	Radius of Wear Track	E_o(mV)	μ	Remarks
1	200	30	0.2465	22	0.70	Original Test
2	100	50	0.2613	18	0.33	New Test
3	100	50	0.250	15	0.28	New Test
4	100	50	0.2031	12	0.28	New Test

The new test runs No. 2, 3 and 4 appear to produce consistent μ values. The average value of friction coefficient is 0.3 with small deviation in any individual run. It is now planned to make further test runs on the CVD coated samples No. 40, 41 and 42 under the same test conditions as in Table 4. However, before proceeding any further it was decided to study the wear track characteristics in the CVD-coated and the plain beryllium samples after the test runs already performed.

The wear tracks were analysed by profilometry using a Dektak profilometer, and the grooves were examined microscopically using the Nomarski technique. The results of these examinations are shown in Figures 3 through 9. In each figure a typical Nomarski image of a groove along with a corresponding Dektak trace is shown. In the Nomarski micrographs, the groves appear flat because of the large depth of focus of the microscope in this mode. All the photographs were taken at 250X magnification. The magnifications in the horizontal direction of the Dektak trace is 200X (2-cm chart paper for 0.01 cm of pin travel on the sample), and 50,000X in the vertical direction (1 cm on chart equals 2000Å of groove depth.

Figures 3 through 9 bring out some interesting observations, which are discussed in the following paragraphs. The overall depths of grooves in both the CVD coated samples and the uncoated beryllium surface are of similar magnitude. However, the walls of the grooves in beryllium are rough and jagged compared to the smooth walls in the wear tracks of CVD coated samples.

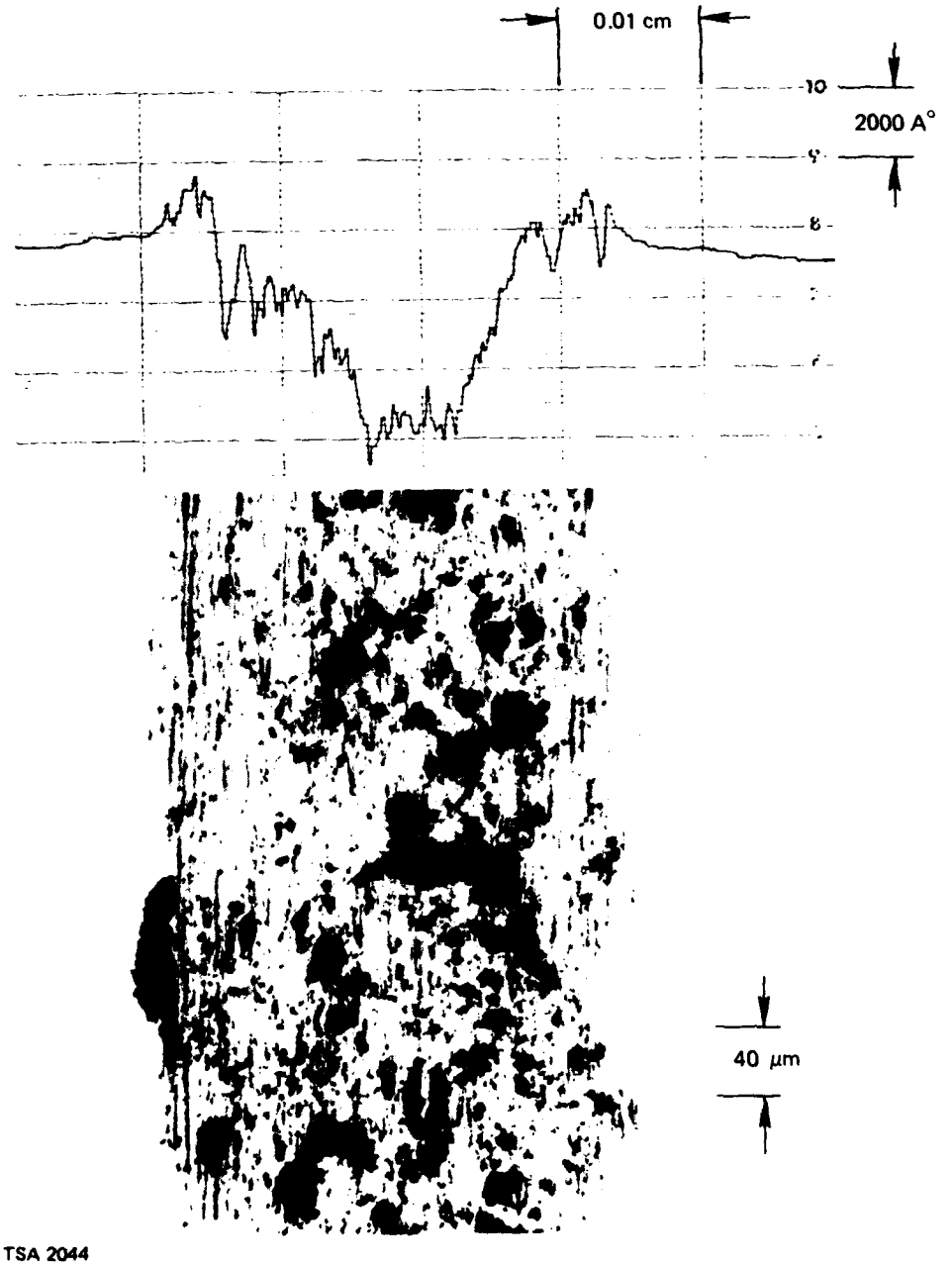

Figure 3. Wear track of run No. 1 on Be sample. 200 r/min, 30-gm load, 5 minutes. Dektak trace at the top and Nomarski picture at the bottom.

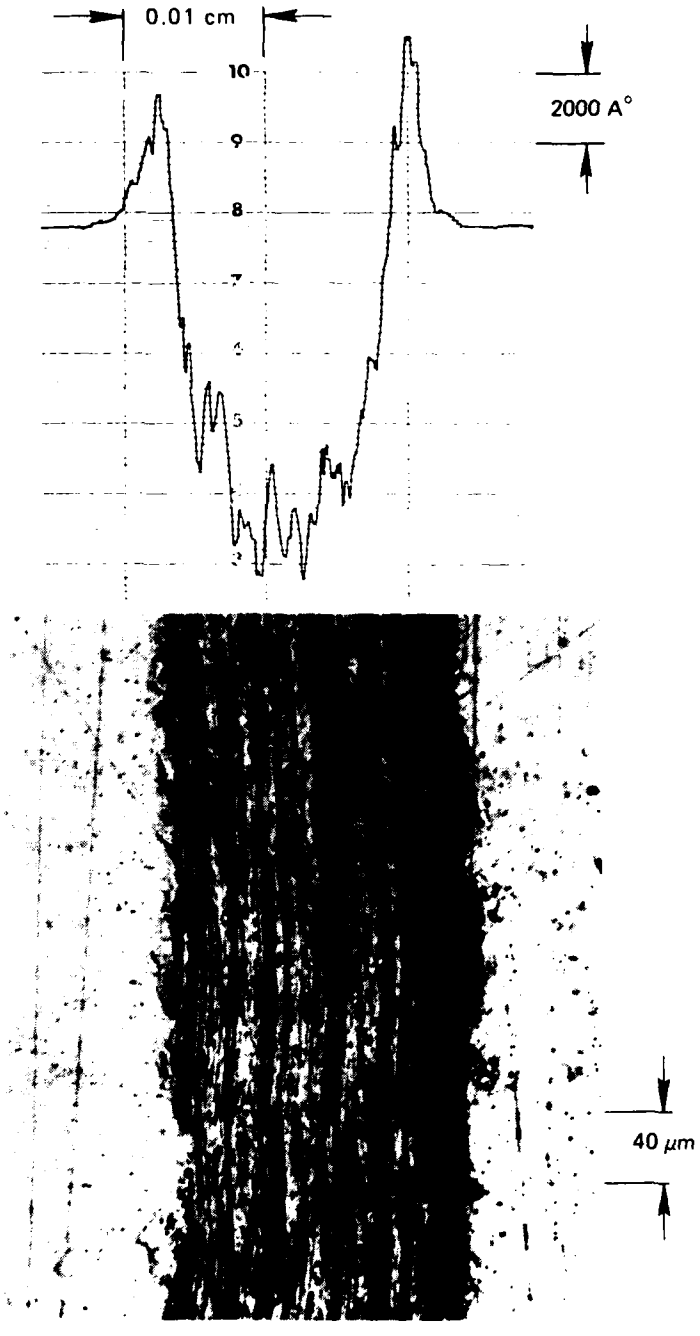

TSA 2045

Figure 4. Wear track for run No. 2 on Be sample. 100 r/min - 10 minutes, 50-gm load. Top: Dektak trace; Bottom: Nomarski picture.

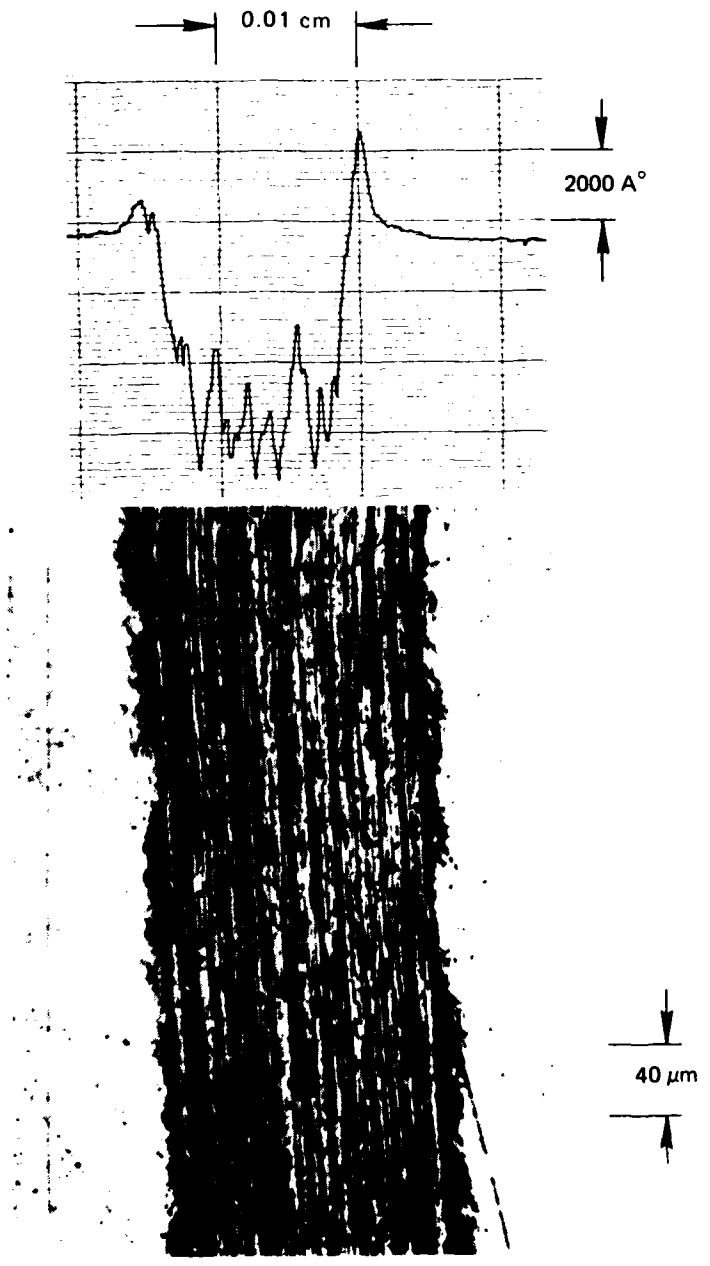

Figure 5. Wear track for run No. 3 on Be sample. 100 r/min - 10 minutes, 50-gm load. Top: Dektak trace; bottom: Nomarski picture.

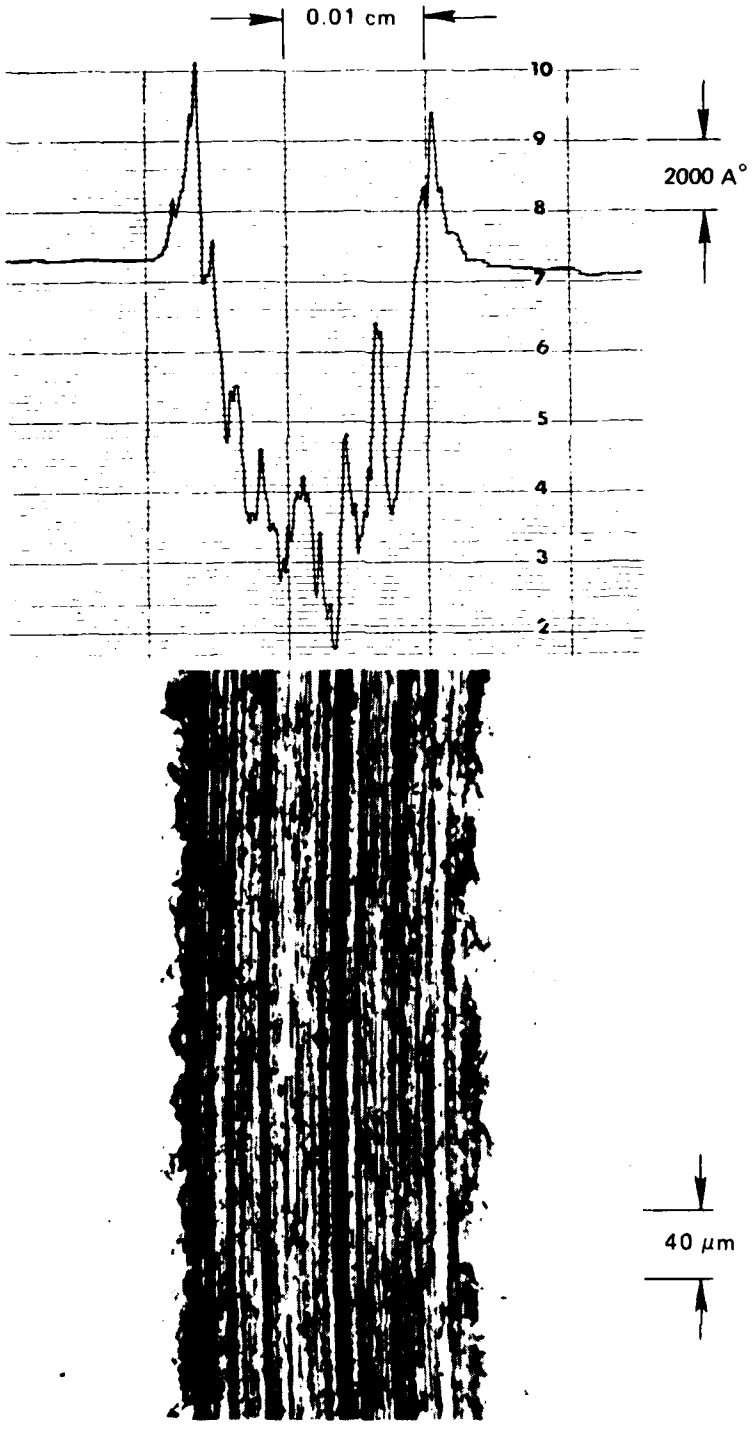

Figure 6. Wear track for run No. 4 on Be sample. 100 r/min - 10 minutes, 50-gm load. Top: Dektak trace; bottom: Nomarski picture (250X).

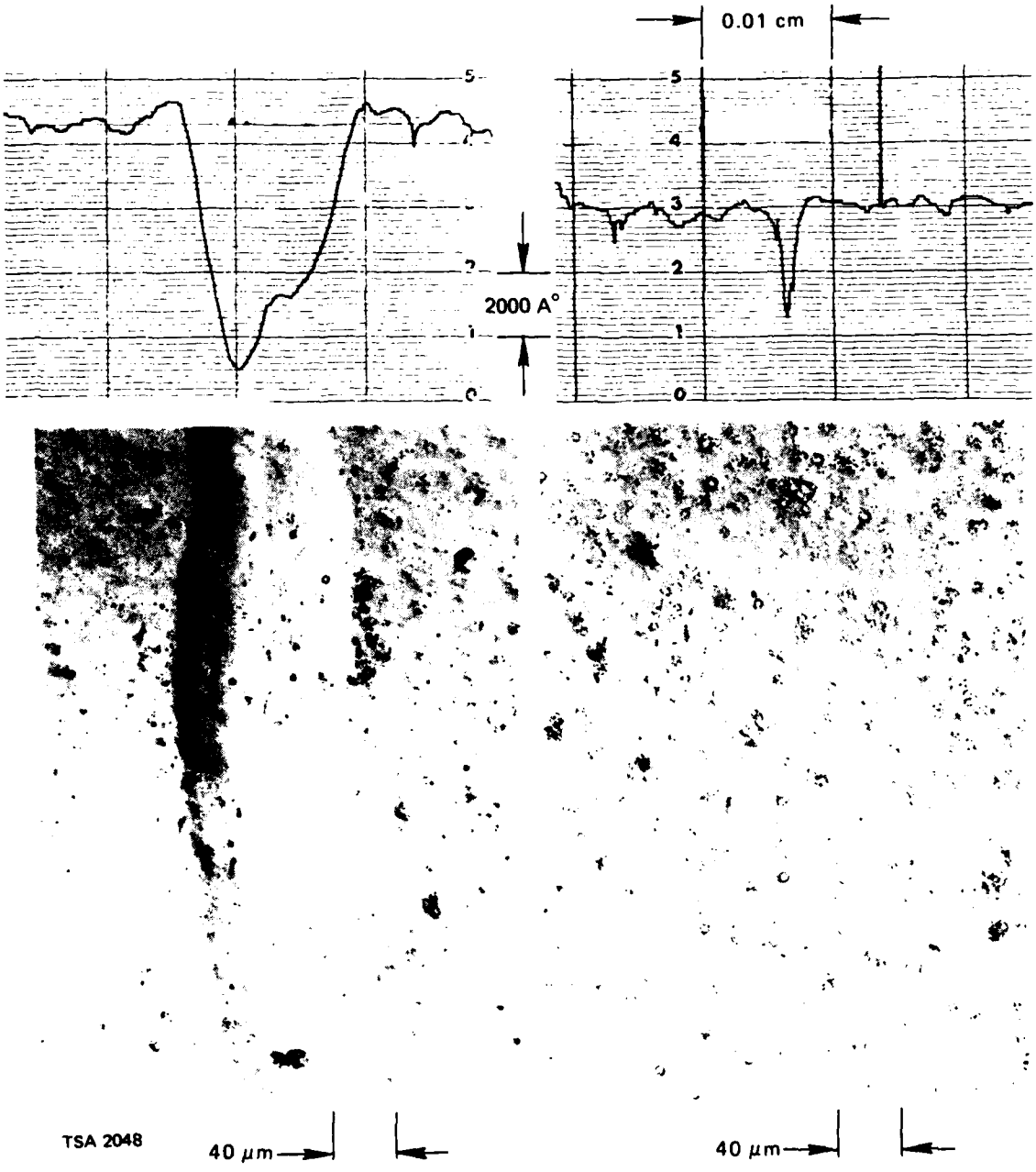

Figure 7. Wear track on CVD sample No. 40 - 200 r/min - 5 minutes, load 30 gm. Left: Top - Dektak trace, bottom - Nomarski picture of sample top. Right: Top - Dektak trace, bottom - Nomarski picture of sample bottom.

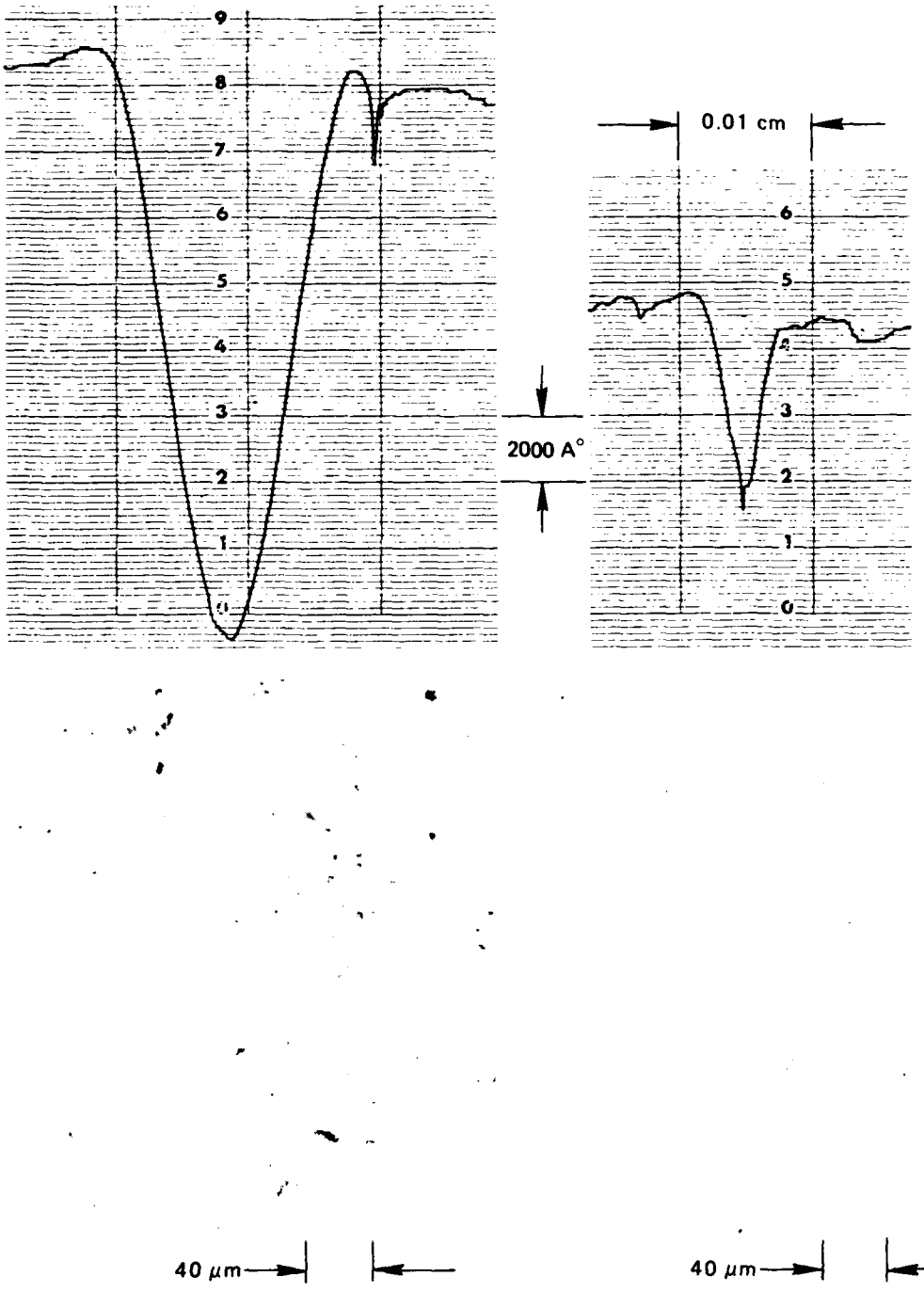

Figure 8. Wear track on CVD sample No. 41 - 200 r/min - 5 minutes, 30-gm load. Left: Top of sample; top - Dektak trace, bottom - Nomarski picture. Right: Bottom of sample; top - Dektak trace, bottom - Nomarski picture.

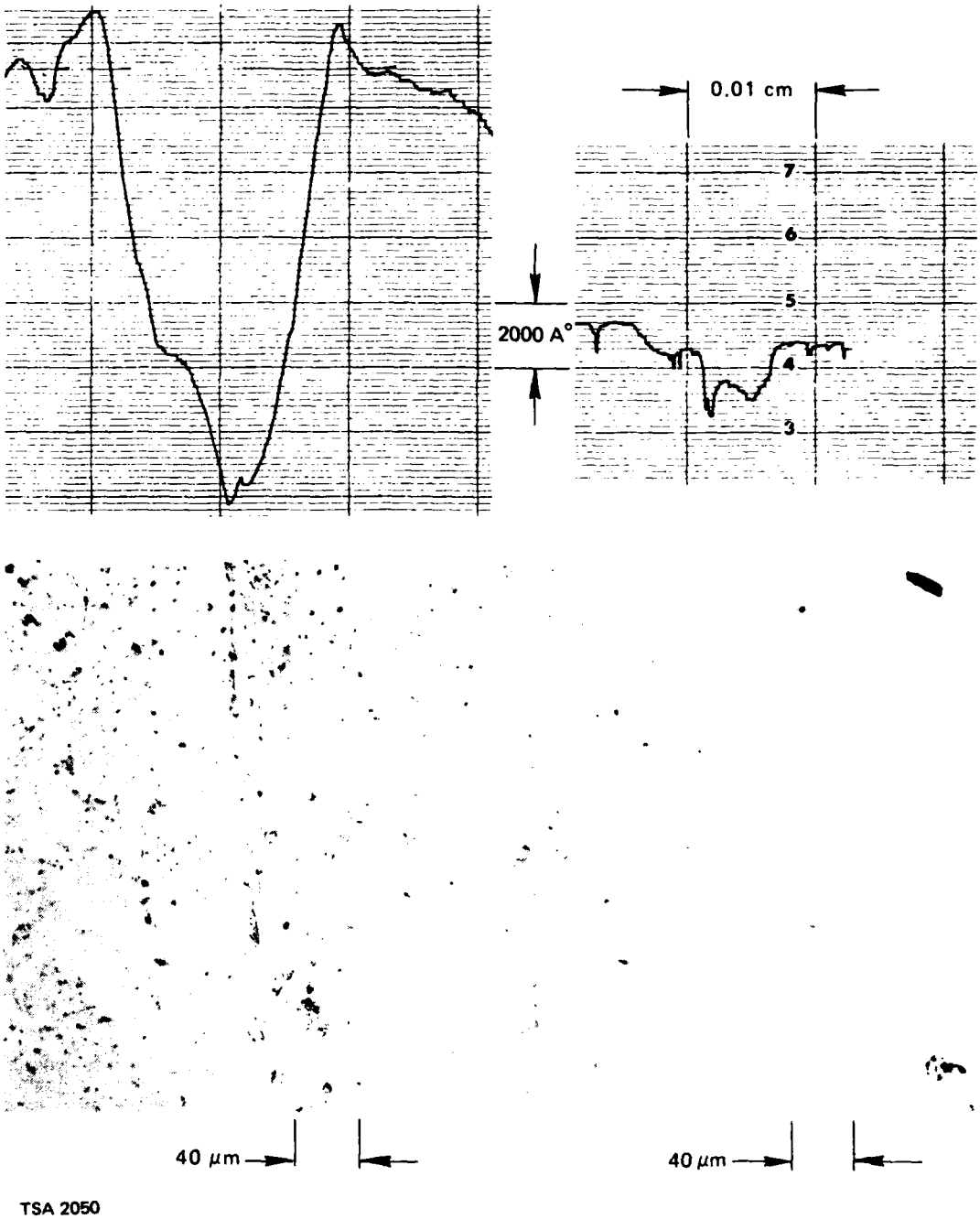

Figure 9. Wear track on CVD sample No. 42 - 200 r/min - 5 minutes, 30-gm load. Left: Top of sample; top - Dektak trace, bottom - Nomarski. Right: Bottom of sample; top - Dektak trace, bottom - Nomarski picture.

Considerable wear debris had obviously formed in the wear tracks of beryllium which had been removed, leaving behind some plowed wear trenches. In the case of the high speed test shown in Figure 3, wear particles much larger than the trenches have been literally sheared off, indicating that the wear testing in this particular case was quite severe.

The trenches in this high-speed test are discontinuous and the width of the groove is larger although the groove is comparatively shallow. This fact can be very clearly seen in the tabulated data in Table 5, of actual groove depths and widths as measured from the Dektak trace of each groove.

Table 5. Measured widths, and calculated and measured depths of wear grooves in beryllium.

Run No.	Test r/min	Depth (μm)	Width (μm)	
			Measured	Calculated
1	200	0.6	275	87
2	100	1.1	170	118
3	100	0.9	170	107
4	100	0.7	155	94

For comparison, the calculated minimum width that should have been obtained in each case is presented in the last column of Table 5. These values wre calculated on the geometrical basis of the dimension of the pin head (the 1/8-inch diameter sapphire ball) and the depth of the grooves as determined from the Dektak trace.

The measured widths in all cases are larger than the theoretical widths. The test runs 2, 3 and 4 at 100 r/min gave, on the average, about 60 percent wider tracks. The 200 r/min run however produced a track more than 3 times larger than the calculated width, which means that there was considerable movement of the pin in the radial direction

during the wear testing which may have been caused by the high rotational speed. That, in turn, may have given rise to the high measured friction coefficient value of 0.7 instead of about 0.3 seen in the lower speed tests. It is therefore reasonable to expect that the friction values for the CVD-coated samples may also be much smaller than the value 0.4 obtained on these samples at the high speed.

The wear track grooves in the CVD-coated samples are remarkably different from those on the uncoated beryllium surfaces. The depths of the grooves on the areas where the coatings are thin are comparable to those on the plane beryllium surface but they are much shallower on the thicker portions of the coatings. Groove depths and width data of the CVD-coated samples, similar to the data on beryllium shown in Table 5, are given in Table 6.

Table 6. Depth and width data of wear tracks on CVD-coated samples of Table 2.

Sample No.	Thin Coating			Thick Coating		
	Depth (μm)	Measured Width (μm)	Calculated Width (μm)	Depth (μm)	Measured Width (μm)	Calculated Width (μm)
40	0.8	150	101	0.3	25	62
41	1.6	190	142	0.6	75	87
42	1.3	200	128	0.3	50	62

For the deeper portion of the grooves, the measured widths are about 50 percent larger than the calculated widths. But in the shallow portion of the grooves the reverse is true. There is no obvious explanation of the latter situation at the moment.

The formation of wear grooves in the CVD coating would tend to indicate that the coating had worn away. But the facts that the groove walls are highly smooth, lack of any plowed trenches and any evidence of wear particle pull-out seem to suggest that there has been no wear of any significance. On that basis the only way to explain the formation of the grooves is that the underlying soft beryllium substrate yielded to form the groove and the CVD film stretched sufficiently to conform to the contour. To further complicate matters, the Dektak trace failed to show the buildup at the edge of the grooves which would be caused by the yielding of the beryllium substrate. An examination of the cross section at high magnification may provide the answer.

The above supposition is further supported by the evidence that the grooves were shallow in the areas where the films are thicker. A positive support of this assumption can come from examining a polished cross section of the groove under high magnification. This is planned as soon as the samples are further wear tested at slower speeds.

3.3.4 Diffusion Anneal of CVD Samples

For limited diffusion studies in the Be-B system using the boron-coated beryllium surface by CVD, the condition of deposition chosen was deposition at 700°C for 2 hours on 3/4-inch diameter polished beryllium discs. A large number of CVD-coated samples were prepared under the above conditions. The samples were cut into half circles along a plane perpendicular to the plane of the films to provide individual samples for each chosen diffusion anneals. Diffusion heat treatments were given at 750°, 800° and 900°C for time periods of 4 hours and 75 hours in high purity helium atmosphere. Details of the diffusion anneal treatments are shown in Table 7.

Table 7. Thermal cycles and visual observation of diffusion anneals.

CVD Sample No.	Heat Treatment	Observations
43 (1/2)	750°C - 4 hrs	Dull gray, peeled at outside edges
43 (1/2)	750°C - 75 hrs	Dull gray, peeled at outside edges
44 (1/2)	800°C - 4 hrs	Shiny blue gray, pink edges, bottom edge peeled
44 (1/2)	800°C - 75 hrs	Shiny steel gray, peeled outside edges
45 (1/2)	850°C - 4 hrs	Shiny steel gray, with some dark gray, bottom peeled
45 (1/2)	850°C - 75 hrs	Shiny steel gray, pink islands, outside edges and bottom peeled
46 (1/2)	900°C - 4 hrs	More than half peeled, pink remaining coating
No 900°C - 75 hr treatment due to extensive peeling at 4 hrs.		

Analytical procedures on the above samples were suspended while awaiting the preparation of stoichiometric Be-B compounds that will be used as standards.

3.3.5 Preparation of Pure Be-B Compounds

The binary Be-B system contains four compounds - Be_4B, Be_2B, BeB_2 and BeB_6. X-ray diffraction patterns of commercially obtained compounds of the above compositions showed all of them to contain very large percentages of BeO. Because of that, the stoichiometry of the commercial compounds were suspected to be incorrect. Early experiments performed at CSDL had shown that these compounds could be formed at relatively low temperatures. It was believed that the oxidation of beryllium could be prevented by fabricating the compounds by HIP processing.

High purity -325 mesh beryllium powder with BeO content of 1.0 percent and -100 mesh crystalline β-boron with 0.2 percent oxygen were used for the preparation of the compounds. Weight percentages for the compositions were calculated for 2.5 gram charges for each of the compounds, making allowances that the existing oxygen in Be and B would end up as BeO. The calculated compositions of the four mixtures were as follows:

(1) BeB_6: 2.20 gm B + 0.31 gm Be

(2) BeB_2: 1.77 gm B + 0.75 gm Be

(3) Be_2B: 0.94 gm B + 1.58 gm Be

(4) Be_4B: 0.58 gm B and 1.93 gm Be

The above four mixtures were individually blended to obtain uniform composition throughout the mixtures. Instead of precompacting these powder mixtures prior to HIPing they were placed inside a well outgassed 1/2-inch ID 1020 steel HIP cannister and tamped in hard. All four mixtures were charged into one cannister, keeping the individual mixtures separated by means of tight fitting stainless steel disc spacers. A cover with a pump-out tube made of 1020 steel was welded on to the cannister. The air inside the cannister was replaced by argon by evacuating and backfilling prior to the welding of the cap to prevent any oxidation of the mixtures during welding. After the welding of the cap, the cannister was evacuated, baked out at 400°C, sealed by pinching and welding the pump-out tube, and then HIPed at 1000°C for 4 hours at 30 kpsi of argon gas.

These HIPed compositions will be homogenized at about 1025°C for 72 hours while still in the cannister. They will then be removed and will serve as standards for both Auger analysis and x-ray diffraction. Microstructure examination and microhardness measurements will also be performed, which will provide guidance to our further studies in the CVD of boron on beryllium.

3.4 Conclusions

High temperature CVD at 850° and 900°C produced hardness values similar to the lower temperature (700° and 800°C) depositions, although at lower indentation loads. The films formed at the higher temperatures are therefore much thinner. Multiphase microstructures were seen on these depositions. Nevertheless, it will be interesting to investigate wear and friction behaviors of these surfaces.

Scaling up to larger size samples presented no special problems, which indicates that the present system is capable of producing CVD coatings on actual gas bearing components of gyros. During these runs it was firmly established that the present CVD process demands a highly clean environment for its success.

It appears that the post CVD heat treatments are capable of yielding limited information on the diffusion kinetics in the Be-B system. However, the same treatments are not likely to produce useful bearing surfaces with Be-B compounds because of the mechanical damage seen as a result of these treatments. If BeB_6 and BeB_2 surfaces cannot be produced during CVD processing then the chances of producing these compounds on the surface seem remote.

In the initial wear tests carried out recently, grooves were found to form which were deep in thinly coated areas and quite shallow on heavier coatings. Measured friction coefficient of 0.4 is quite high but the high values measured may have been due to the high speed used during these preliminary tests. Lower speed measurements will be performed on the same samples and it is possible that the true friction coefficient may be much less than 0.4. In spite of the deep grooves that were formed, the coating appears to be resistant to large scale debris generation as evidenced by the smoothness of the groove walls and the minimal mechanical damage to the coating in the grooves (no plowing or pullouts were seen).

Due to convection currents, the CVD coating is heavier at the bottom parts of the surface with gradual decrease of thickness to the top. It would be highly desirable to have uniform thickness throughout the coating. Therefore it is now planned that the sample be rotated about its axis during the CVD process at a speed of between 5 and 10 r/min.

SECTION 4

ION IMPLANTATION

4.1 Introduction

Boron ion implantation into the beryllium surface is being investigated as a means of producing hard, wear-resisting surfaces which have potential for gas bearing use. Case hardening or surface alloying of materials by this process is an emerging technology that has borrowed heavily from semiconductor electronic device fabrication, where the process is fully mature. While the basic concepts are similar, in practice the metallurgical modification of material requires much greater doses than are required to alter the electronic characteristics of a semiconductor. That difference and others makes this an exploratory effort, not only in the evaluation of results but also in the development of processing and testing procedures.

4.2 Process Description

The ion implantation process differs from those based on diffusion by employing kinetic, rather than thermal, energy to introduce and emplace the foreign species which is intended to modify the host material. A high kinetic energy is given to the species to be implanted, such as boron, by first ionizing the boron and then accelerating the ions through an electrical potential difference. They are then directed as a beam or current of ions onto a substrate material, such as beryllium, whose surface their high kinetic energy allows them to penetrate. The quantity or dose of boron delivered is determined by the magnitude of the current and the length of time it is applied. The range of penetration of the ions depends on the accelerating potential.

Consequently, for ion implantation processing, the concentration of boron in the surface of the beryllium is not limited by its solubility, and the penetration of boron into the beryllium is not restricted either by the diffusivity of the boron or by the presence of a native oxide film on the beryllium. A principal feature of ion implantation is therefore the unique degree of control which it affords in generating alloyed surface layers.

4.3 Previous Work

Experiments performed on beryllium samples implanted with boron concentrations in the range of 10 to 40 atomic percent at the Naval Research Laboratory (NRL) in a low current machine (so that the processing time requirement was inordinately long) showed that significant boron concentrations could be attained in the beryllium surfaces. Two independent methods of assessing erosion due to sputtering indicated that it was negligible and therefore did not set any serious limits on the concentrations which might be reached. These studies also demonstrated that increases in hardness values occurred with implantation and these values increased further when the samples were subjected to post-implant heat treatments.

Subsequent work on a second group of specimens, which were each of a size (3/4-inch diameter) large enough to permit friction and wear testing after implantation, was performed in a new implanter whose higher current capability made it a credible metallurgical tool. These were implanted to levels of 60 and 40 atomic percent boron in beryllium and again showed hardness increases. However, inconsistencies and a lack of reproducibility showed the need for better sample thermal control during implantation and examination of more than a single sample of a given type.

Much of the earlier friction and wear testing in this part of the program was done in a pin-on-disc format with pins of a material commonly used for this purpose, 52-100 steel. The tests were performed on freshly cleaned surfaces without lubricants or coolants, as a means of ensuring well defined and reproducible conditions. Perhaps because of the absence of any lubricating film, in many instances the steel pin material "crayoned" itself onto the disc surfaces resulting eventually in steel rubbing on steel. This occurrence, plus the desire to generate data with more direct engineering value, led to the recommendation that further wear and friction evaluation be performed with an aluminum oxide (sapphire) tipped pin.

An interesting observation made during these earlier evaluations was the increased wear resistance imparted to the surface by the implantation (versus the hardened steel pin) even when no substantial increase in hardness was measured by conventional means for the very thin implanted layer.

Microstructure evaluations of the implanted layers were attempted using reflection electron diffraction (RED) when it was realized that use of the transmission electron microscopy (TEM) and diffraction technique could pose some logistical problems. The results obtained by RED were termed inconclusive in that no clear diffraction pattern was obtained from the surface. The absence of a diffraction pattern was initially interpreted as showing that

(1) the surface was rendered amorphous as a consequence of implantation, or

(2) metallic surface and/or beryllium boride compounds were covered over with a thin oxide film which (especially with boron present) might be glassy and amorphous or

(3) both of the above

Subsequent RED examinations of as-polished, unimplanted beryllium also showed the absence of a diffraction pattern; however, the existence of a well-defined beryllium pattern was clearly observed when the unimplanted beryllium sample was stress relieved for 1 hour at about 790°C. This clearly suggested that the observed amorphous nature of the surface in the implanted specimens might well be the result of the sample preparation procedure that was adopted prior to implantation of the specimens and may or may not be related to the implantation of the boron species.

4.4 Present Work

4.4.1 Sample Preparation

Several of the as-polished discs (which were produced following a stress-relieving heat treatment of the machined beryllium discs)[11] were selected for additional implantation. Some of these were implanted at a local vendors facility, identified as samples LV1-4 while others were processed at the Naval Research Laboratory. Samples in the former lot included variations such as 40 atomic percent single dose, double-dose (including high energy/low dose and low energy/high dose) and graded layer implants. In one instance pulsed electron beam annealing of a boron film on beryllium was also attempted. In each instance, however, the appearance of a severely oxidized surface was observed following the processing.

Samples implanted at NRL, on the other hand, appeared quite satisfactory. These were identified with the prefix NRL, as indicated in Table 8. In this latter case samples were processed for both flat and graded profiles at peak 40 atomic percent. It was suspected that a poor vacuum and insufficient temperature control at the substrate were the cause of the severe oxidation observed for the first batch of samples. The different parameters used for these various samples are shown in Table 8.

Table 8. Implantation parameters for LV* and NRL** implanted samples.

Specimen No.	Peak Nominal Concentration (atom %)	Type of Implantation	Heat Sinking at Substrate	No. of Doses	Energy Range (keV)	Depth (in Å)
LV 1	40	Single dose	Poor	1	50	2150
LV 2	Not Applicable (NA)	Boron film; pulsed electron beam	None	NA	NA	NA
LV 3	40	High energy/ low dose + low energy/ high dose	Poor	2	50; 200	2150; 6800
LV 4	40	Graded	Poor	6	10-50	430-2150
NRL 40-IV	40	Uniform	Good	6	25-192	1000-6600
NRL 40-V	40	Uniform	Good	6	25-192	1000-6600
NRL 40-VI	40	Graded	Good	6	25-192	1000-6600
NRL 40-VII	40	Graded	Good	6	25-192	1000-6600

*LV = Local Vendor
**NRL = Naval Research Laboratory

4.4.2 Optical Microscopy

Figure 10 shows a typical view towards the edge of an NRL-produced 40 atomic percent boron implanted beryllium disc sample. In the process of holding the specimen firmly inside the holder during implantation, regions close to the edge of the disc are partly covered. This, therefore, results in boron implantation into most, but not all, of the sample surface.

The view in Figure 10(A) shows both the implanted and the unimplanted area. It is interesting to note the level of considerably increased detail in the grain structure (boundaries, twins) that are observed in the implanted regions compared to the unimplanted regions. This obviously indicates that although substantial removal of beryllium from the surface does not occur during boron implantation (as has been demonstrated earlier),[12,13] the surface is nevertheless gradually etched by the incident ion beam.

It should be noted that whereas these effects were clearly visible when the sample was examined using the differential phase contrast (Nomarski) technique, these details were lost when the sample was examined using the more conventional procedure of polarized light microscopy which is the technique used in most cases for the optical examination of the microstructures of beryllium.

4.4.3 Chemical Analyses

Because of the many difficulties encountered earlier with obtaining sharp, well-defined diffraction patterns using RED with the view of providing detailed information on beryllium-boron compound formation in the implanted layers, subsequent efforts were mainly directed at examining the implanted materials using the Rutherford Back Scattering (RBS) and the Auger Electron Spectroscopy (AES) techniques for chemical composition analysis. Since both these techniques are capable of determining composition depth profiles, they were both

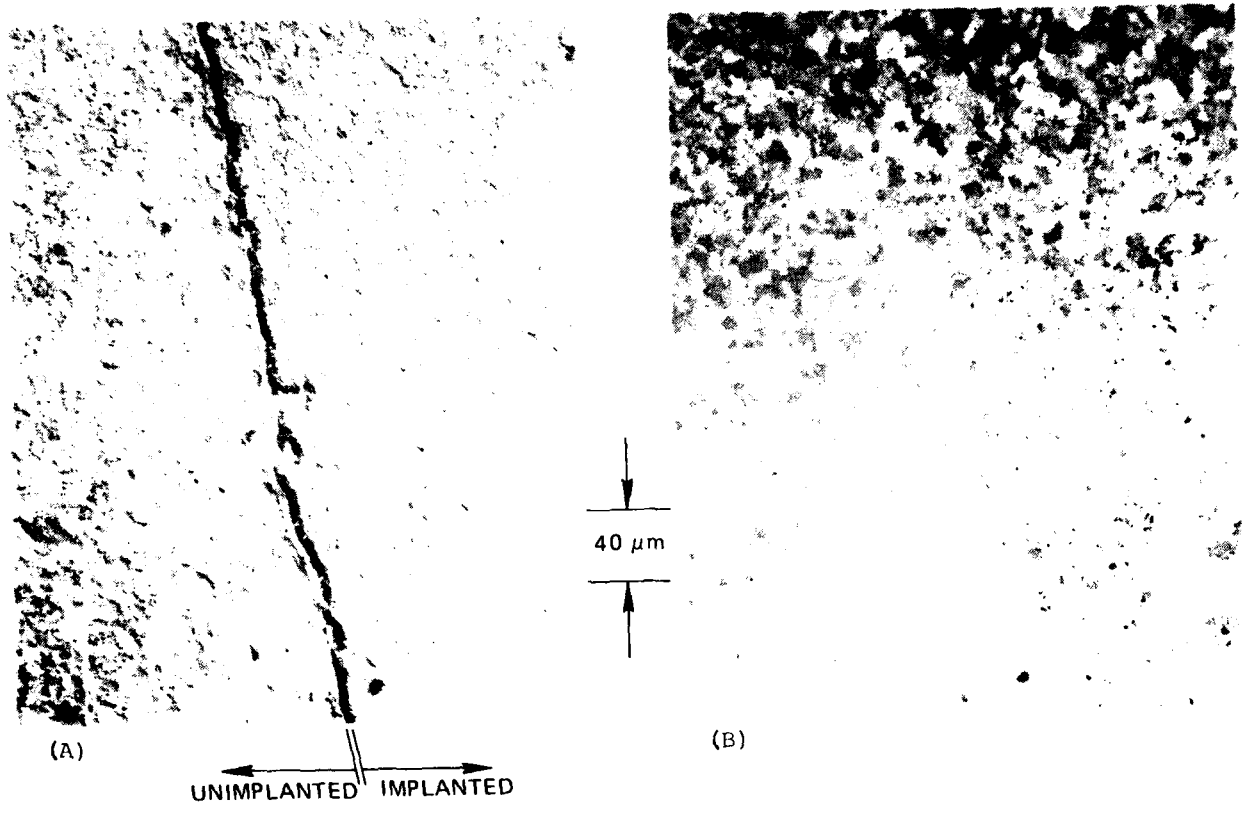

TSA 2051

Figure 10. Micrographs showing (A) Etching of sample NRL 40-VI from the implantation process, Nomarski, and (B) polarized light micrograph of the same region showing grain structure.

pursued with the aim of establishing correlations between the use of these two different analytical procedures. The RBS data included in this report were collected at the Naval Research Laboratory and part of it was reported recently in a joint paper between NRL and CSDL.[14] AES, however, was performed locally under CSDL direction.

4.4.3.1 Experimental Details

4.4.3.1.1 Rutherford Back Scattering (RBS)

Rutherford back scattering was performed using 3-MeV alpha particles incident at 45 degrees to the surface normal and at 90 degrees to the detector. Because the kinematical scattering factors for boron and beryllium do not differ sufficiently to separate the signal due to the deeply buried boron from that due to the near surface beryllium, the determination of the boron profile involved more elaborate techniques. First, a spectrum from an unimplanted specimen was subtracted from the spectra of the implanted samples. (The resulting difference spectrum had the advantage of being less sensitive to the choice of beryllium cross section.) Then, an RBS simulation computer code was used to generate a theoretical difference spectrum which was compared to the observed difference spectrum. The matching process involves adjusting the concentration profile input to the code until the best fit to the observed data is achieved. The final form of the profiles for the flat and graded distributions of the NRL samples are shown in Figure 11.

It is estimated that the uncertainty in the boron concentration is 15 to 20 percent of the plotted values. The depth scale is less certain since the back scattering technique is sensitive only to the number of boron atoms per atoms-per-unit area and is insensitive to the local atomic density. It is expected, therefore, that the true distributions may differ from those in Figure 11 by some expansion or contraction along the depth axis.

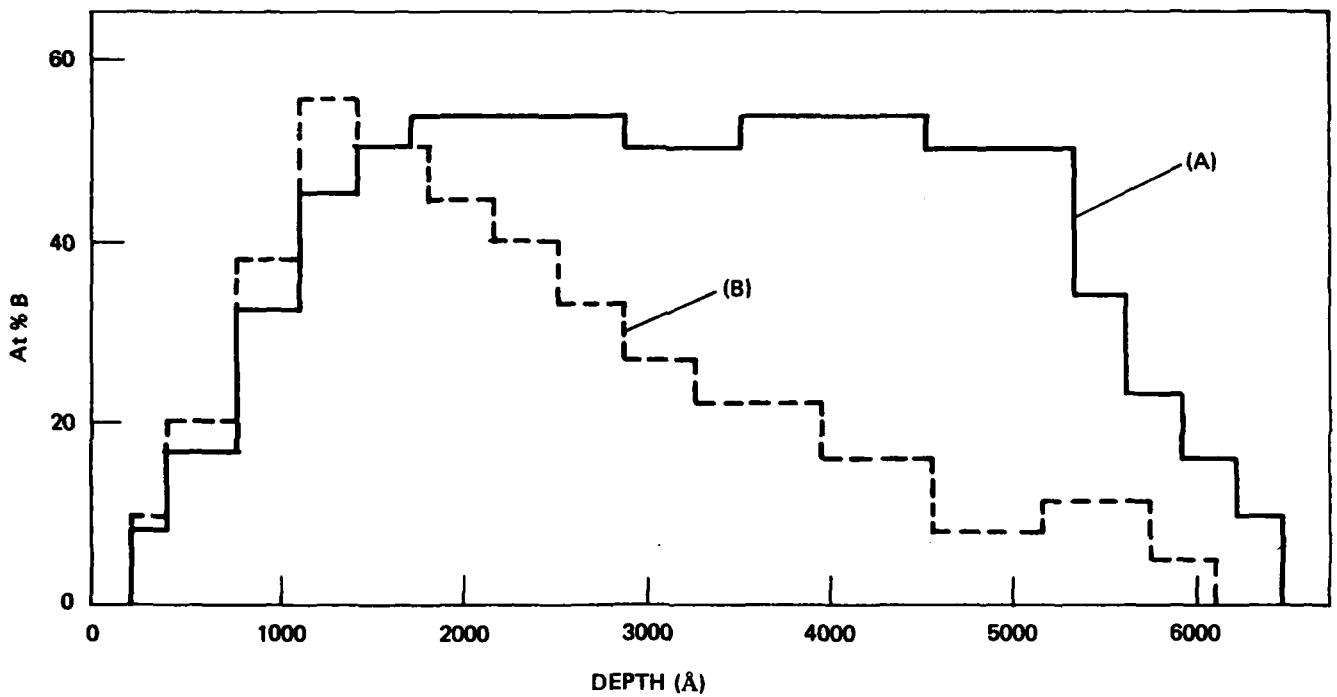

Figure 11. RBS concentration profiles of (A) flat NRL 40-V, and (B) graded layer NRL 40-VI samples.

4.4.3.1.2 Auger Electron Spectroscopy (AES)

Auger evaluation of the implanted materials was performed using a Physical Electronics Model 590 machine. The machine was operated at 5 kV and the spot size of the incident electron beam was slightly less than about 1 μm. Depth profiles were obtained by sputtering the sample with argon ions and simultaneously examining the chemical composition of the material that was exposed to the incident beam at the various depths. The data was plotted on a chart recorder with the concentration (as indicated by the peak-to-peak amplitude) of the several atomic species of interest on the vertical (y) axis and the time of sputtering on the horizontal (x) axis. Since the rate of sputtering of the implanted layer was not known, it was not possible to relate the time of sputtering to the depth attained inside the sample by simple conversion of the data.

To more accurately determine the concentration profile, an alternate method was devised. This consisted of measuring the depth of the groove (that was formed by sputtering of the sample surface) with a Sloan Dektak surface profilometer and assuming that the rate of sputtering was a constant throughout the sputtering period. A given fraction of the groove depth was, therefore, equivalent to the same fraction of the sputtering time.

4.4.3.2 Results

Since all of the samples in the LV series clearly appeared to be severely oxidized, their value from the point of view of evaluation as a potential gas bearing surface was considered minimal at best. The graded composition sample LV-4 was, nevertheless, evaluated further to determine if indeed the anticipated profile was actually achieved. It was hoped that if the profile could indeed be achieved using the processing parameters used at the local vendor's facility, then useful samples which do not show severe oxidation could hopefully be procured at a later date by assuring that all implantation processing was performed under the correct conditions of vacuum and substrate temperature control.

The RBS and AES data obtained on the LV-4 sample is shown in Figures 12 and 13. A close correlation in the profiles was obtained by these two different techniques. The profile at any given depth was considered to be more truly represented by the AES data in that a substantial uncertainty was suspected in the RBS data relative to actual depth (for the reasons outlined earlier). The absolute value of the atomic concentration was, however, deduced from the RBS data with which a higher level of certainty was believed to be associated. The AES signal was normalized to give the spectra that is shown in Figure 13. Such a normalization procedure is somewhat suspect in that the sputtering rates of B and Be and their effect on the Auger electron signal was not known.

It should be noted that the shape of the depth profile is much the same in both cases and that these measurements also indicate a flat boron profile as opposed to the graded one that was anticipated. An additional feature of the AES data obtained on this sample was a very high level of oxygen present at the surface, possible as BeO. (In each of the implanted specimens that were examined, the boron-containing layer was observed to be buried inside the beryllium in that the beryllium concentration decreased from the surface into the implanted layer and increased again as the beryllium bulk underneath the boron implanted layer was approached.)

AES profiles measured for NRL implanted peak 40 atomic percent flat and graded profile specimens are shown in Figures 14 and 15. The measured profiles were close to what was expected on the basis of the RBS data shown in Figure 11. These data were not normalized because of the reason discussed above (regarding lack of information on the relative sputtering rates of B and Be) and are presented in the raw form. It should be noted from Table 8 that the flat and graded samples evaluated using RBS in Figure 11 were identically processed to those

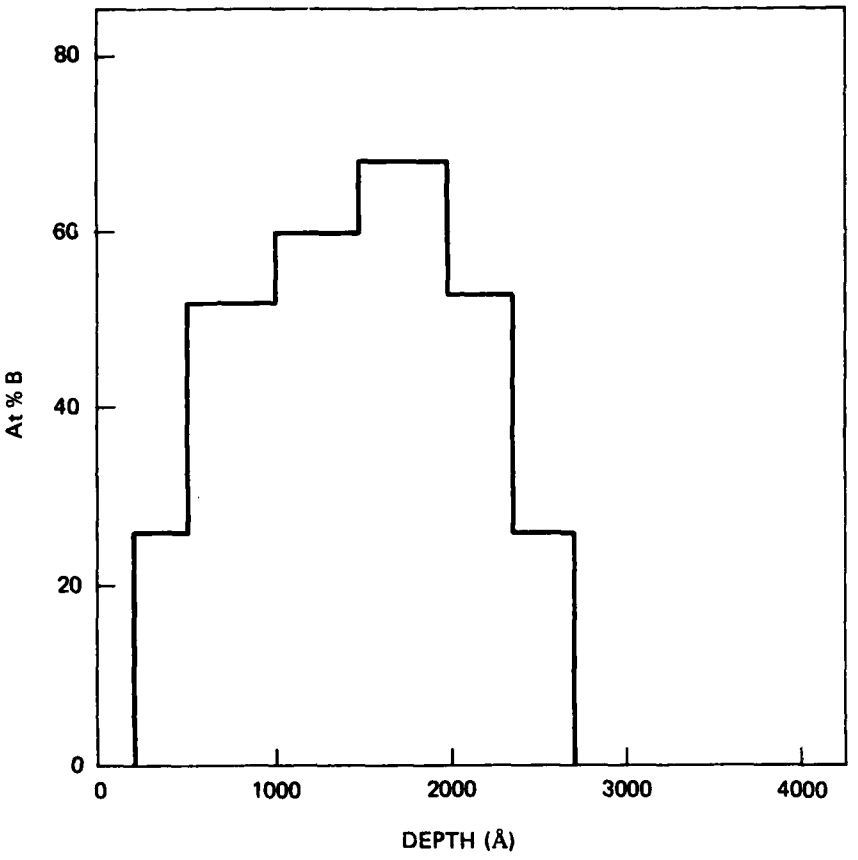

Figure 12. RBS concentration profile of LV4 sample.

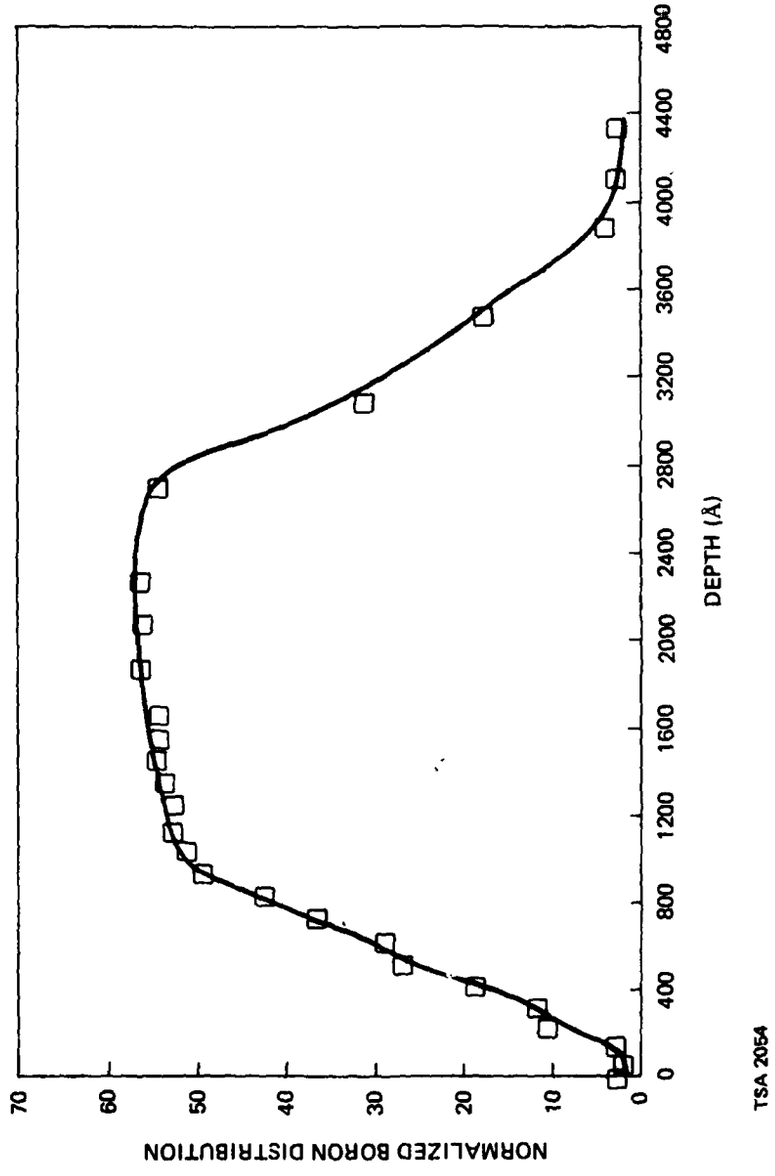

Figure 13. AES concentration profile of LV4 sample.

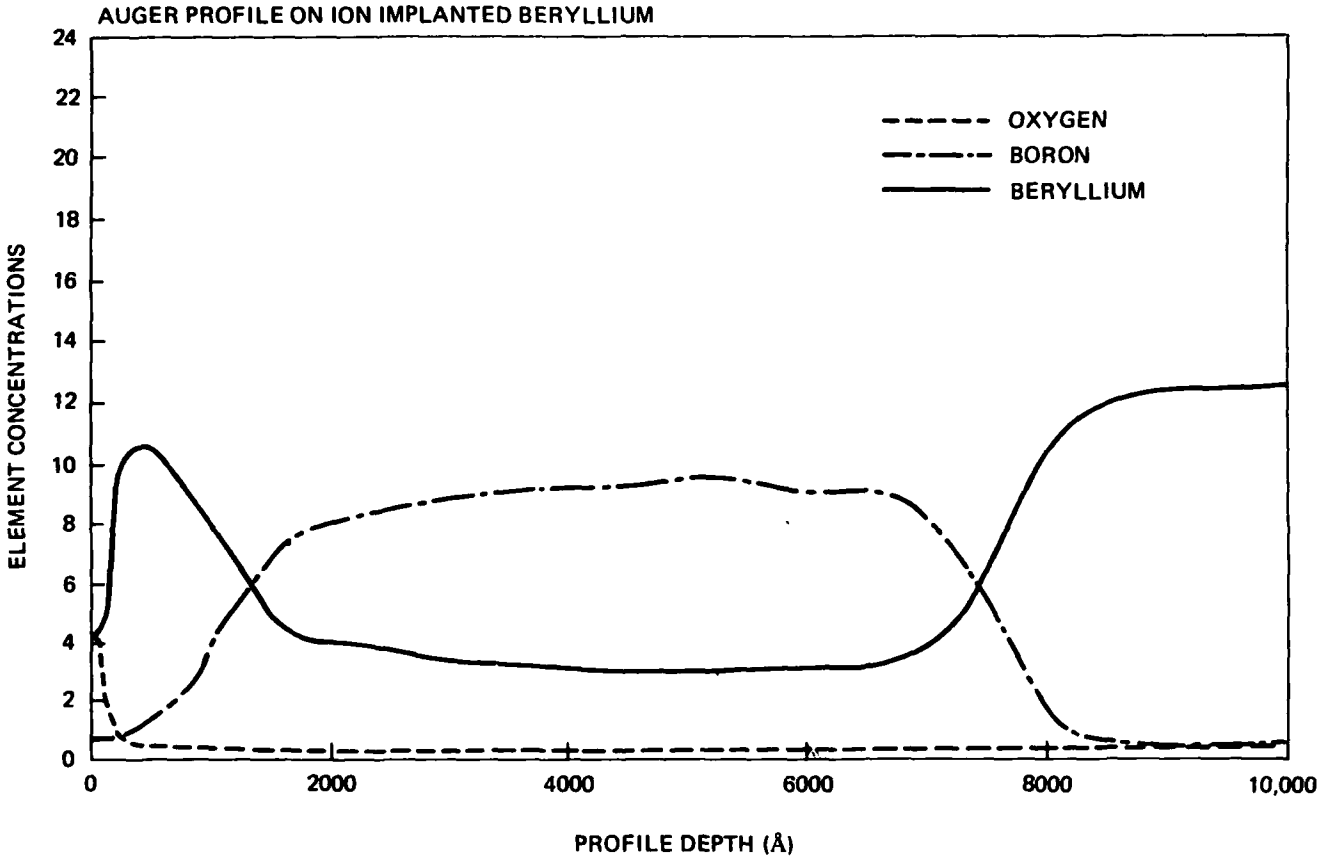

Figure 14. Depth concentration profile of NRL flat distribution sample (NRL 40-IV).

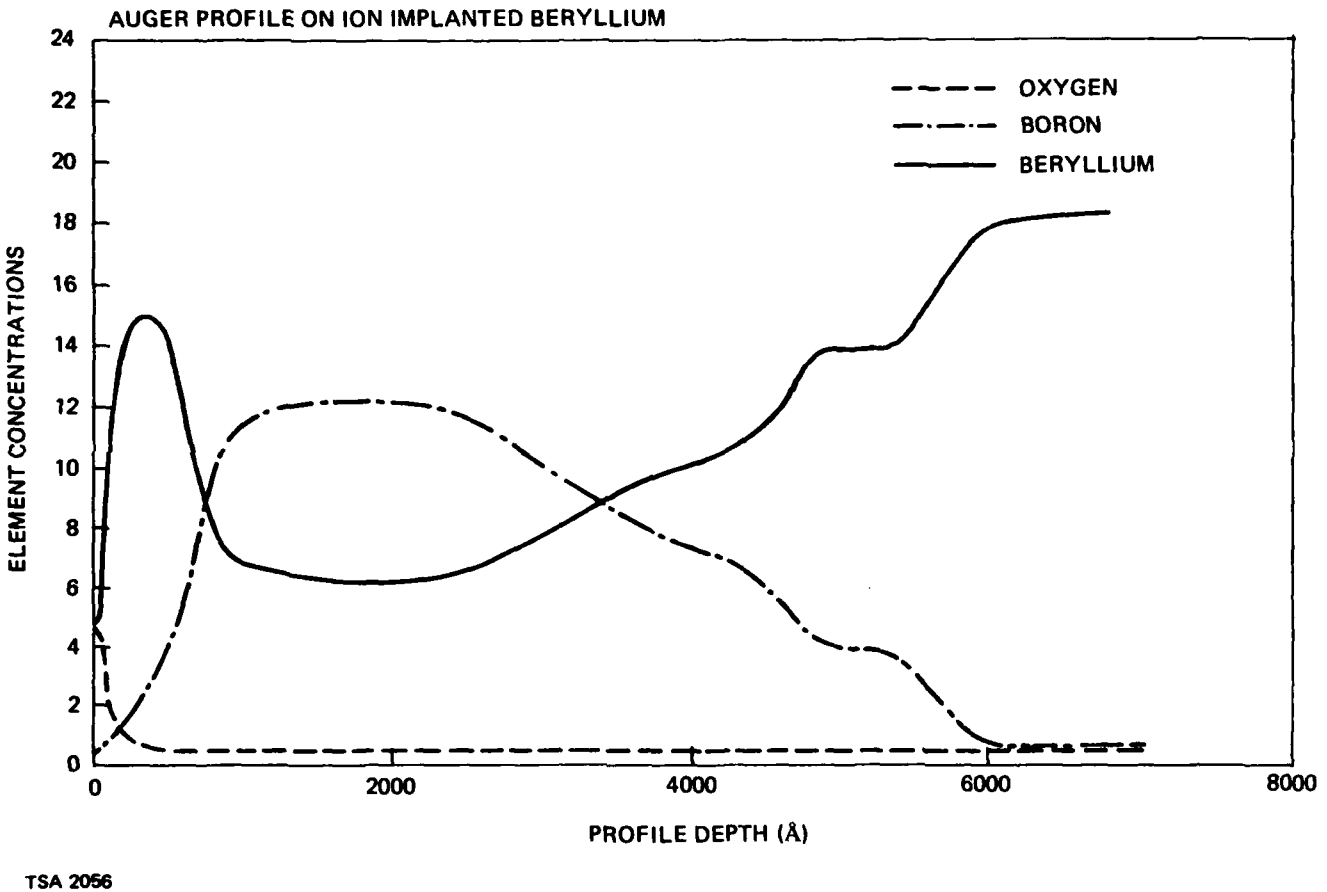

Figure 15. Depth concentration profile of NRL graded distribution sample (NRL 40-VII).

evaluated using AES in Figures 14 and 15. Once again, a close correlation was observed between the RBS and the AES data, clearly establishing a feasibility of ultimately using AES (which is more accessible) for determining as-implanted and post-implant heat treated profiles in these specimens.

It should be noted that in all the samples that were examined, the actual boron atomic concentration was measured substantially higher than the intended concentration which was expected from theoretical considerations.

4.4.4 Friction and Wear Testing

Unlike all of the previously reported data on implanted materials, which were collected elsewhere, the testing discussed in this section was performed on an in-house CSDL flex-pivot wear-tester that was specifically designed and built for this purpose. A brief description of the capability of this apparatus and the data that were collected are given below. A more detailed description of this equipment is given in Reference 10.

4.4.4.1 Apparatus

An overall view of the flex-pivot wear-tester is shown in Figure 16. This apparatus was designed for maximum adaptibility and is capable of performing both pin-on-disc and disc-on-disc type of wear tests. Loading can be varied from a few grams to 10 kilograms by means of either dead weights or a pneumatic loading device. A signal generator coupled to an elastic flex-pivot provides a continuous torque signal from which the value of the friction coefficient can be calculated. Test speed can be varied from 100 to 1200 r/min. This test equipment is installed in a beryllium hood to permit tests on beryllium containing metals and ceramics.

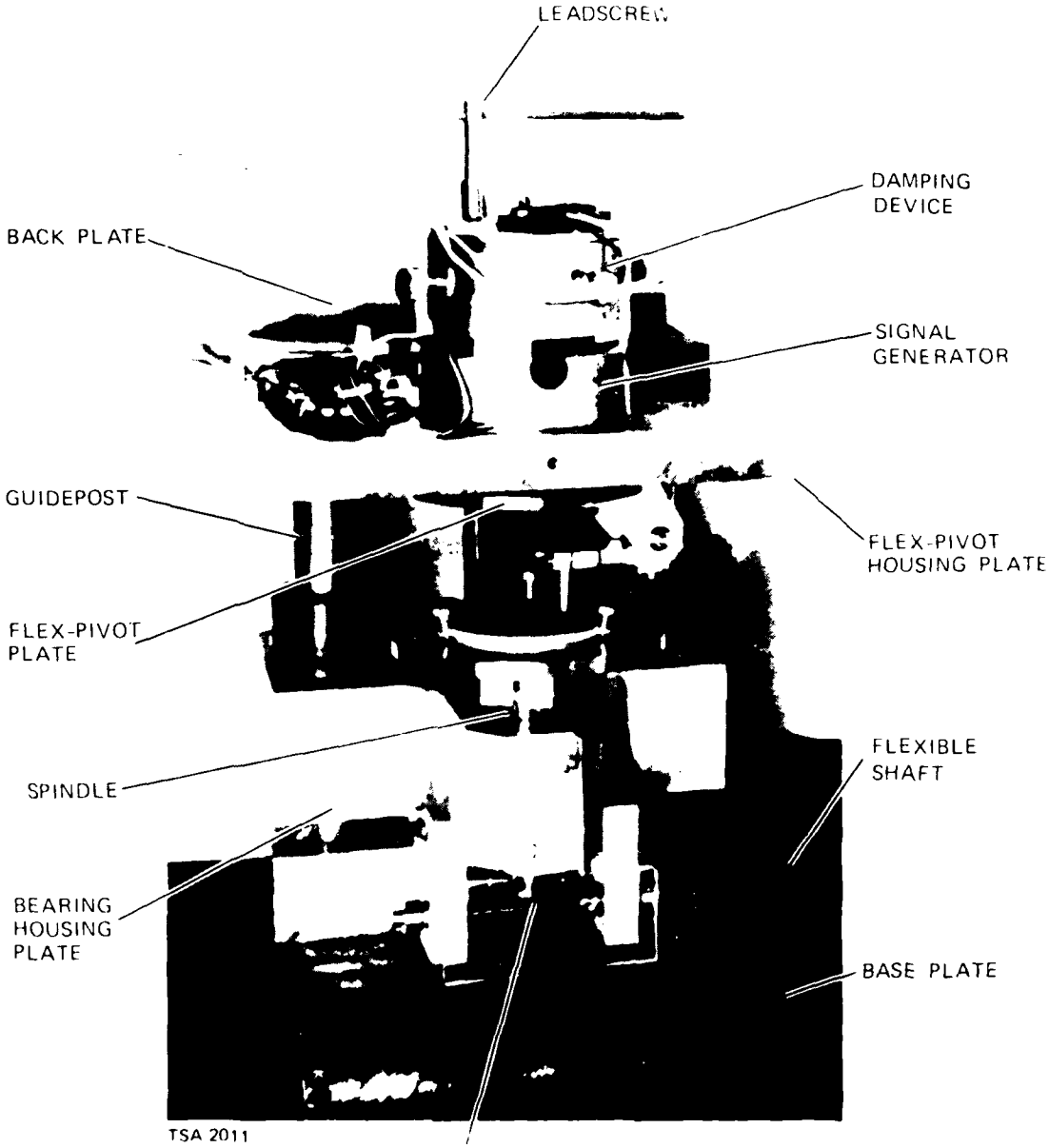
LEADSCREW
DAMPING DEVICE
BACK PLATE
SIGNAL GENERATOR
GUIDEPOST
FLEX-PIVOT HOUSING PLATE
FLEX-PIVOT PLATE
FLEXIBLE SHAFT
SPINDLE
BEARING HOUSING PLATE
BASE PLATE
TSA 2011
BEVEL GEARS

The basic design of the apparatus includes the measurement of torque using a Bendix double-reed flex-pivot, which is basically a linearly-elastic torsional spring. The angular deflection of this flex-pivot is proportional to the torque associated with the friction process. The flex-pivot plate, serves as an attachment point for the stationary specimen holders. The opposite end of the flex-pivot holds a microsyn signal generator rotor, permitting the measurement of the angular deflection.

4.4.4.2 Results

All the testing was performed in a pin-on-disc geometry with a 1/8-inch sapphire ball serving as a pin. The testing was performed in an ambient air environment and no lubrication was provided during this testing. Loads were varied between 20 and 60 gm and the samples were rotated at 100 r/min with linear speeds ranging from 75 to about 95 mm/sec. (This depended on the exact location of the pin.) The values of the friction coefficient were not expected to shown any appreciable differences over such a small variation in linear speed. (This was independently verified experimentally by slightly varying the r/min with the pin in a given location, and noting that no significant change occured in the value of the torque readout.)

Most of the effort was concentrated on determining the differences between flat profile samples and graded profile samples with peak boron concentration values of nominally 40 atom percent. (RBS data shown in Figure 11 had indicated a substantially high peak boron atomic concentration for these materials.) The time of test in each instance was 10 minutes during which the friction data was recorded continuously on a chart recorder. After the testing, samples were removed from the apparatus, the wear track was photographed optically using the Nomarski technique and the surface profile across the wear track was determined with a Sloan Dektak profilometer.

A large number of friction runs were performed on one sample of the graded variety and one of the flat profile type. These runs were performed to examine the scatter in the data and to gain a high level of confidence in the results that were obtained for the friction values. The friction coefficient was evaluated for different times at different values of the applied loads. The values calculated from several friction traces for the different samples are shown in Tables 9 and 10. Good agreement was observed from run to run, especially for a given low (20-g) load.

The friction traces obtained on these samples at varying loads were quite interesting. As shown in Figure 17, the traces obtained at the low loads showed little variation of the friction coefficient with time. These traces were somewhat similar to those obtained on polished unimplanted beryllium excepting that the traces on the latter indicated a substantially larger stick slip behavior.

The friction traces obtained at the higher loads on these samples, however, showed a marked deviation from the flat type trace observed for beryllium and for the implanted specimens at the low loads. In these cases, three almost distinct regions were indicated as shown schematically in Figure 18. These were interpreted as those corresponding to a region with low/no wear (friction coefficient constant), a region with rapidly increasing wear as indicated by the accompanying increase in the friction coefficient, and a steady state wear region where the friction coefficient value increases quite gradually. As shown schematically in this figure, this effect is more pronounced at the higher loads. Both regions A and B shrink with increases in applied loads.

The physical processes belie to be responsible for these observations are those related to the ,adual wearing away of the ion implanted layer with time. It is suspected that at high loads and at very long times, the friction characteristics of beryllium will be approached in each of these instances.

Table 9. Friction coefficient data on NRL 40-IV; calculated at different times.

Run No.	Load (g)	Time (minutes)				
		.1	1	3	5	10
1	20	.13	.13	.15	.22	-
2	20	.11	.11	.13	.20	-
3	20	.20	.20	.26	.35	-
4	20	.15	.15	.22	.35	-
5	20	.13	.11	.15	.22	-
6	20	.18	.18	.20	.31	-
7	45	.13	.20	.33	-	-
8	45	.18	.22	.48	.66	.90

Table 10. Friction coefficient data on NRL 40-VII; calculated at different times.

Run No.	Load (g)	Time (minutes)				
		.1	1	3	5	10
1	20	.07	.11	.11	.11	.20
2	20	.26	.31	.35	.46	.48
3	20	.22	.29	.29	.33	.37
4	20	.09	.13	.13	.18	.20
5	45	.24	-	.40	.55	-
6	45	.26	.31	.40	.55	-

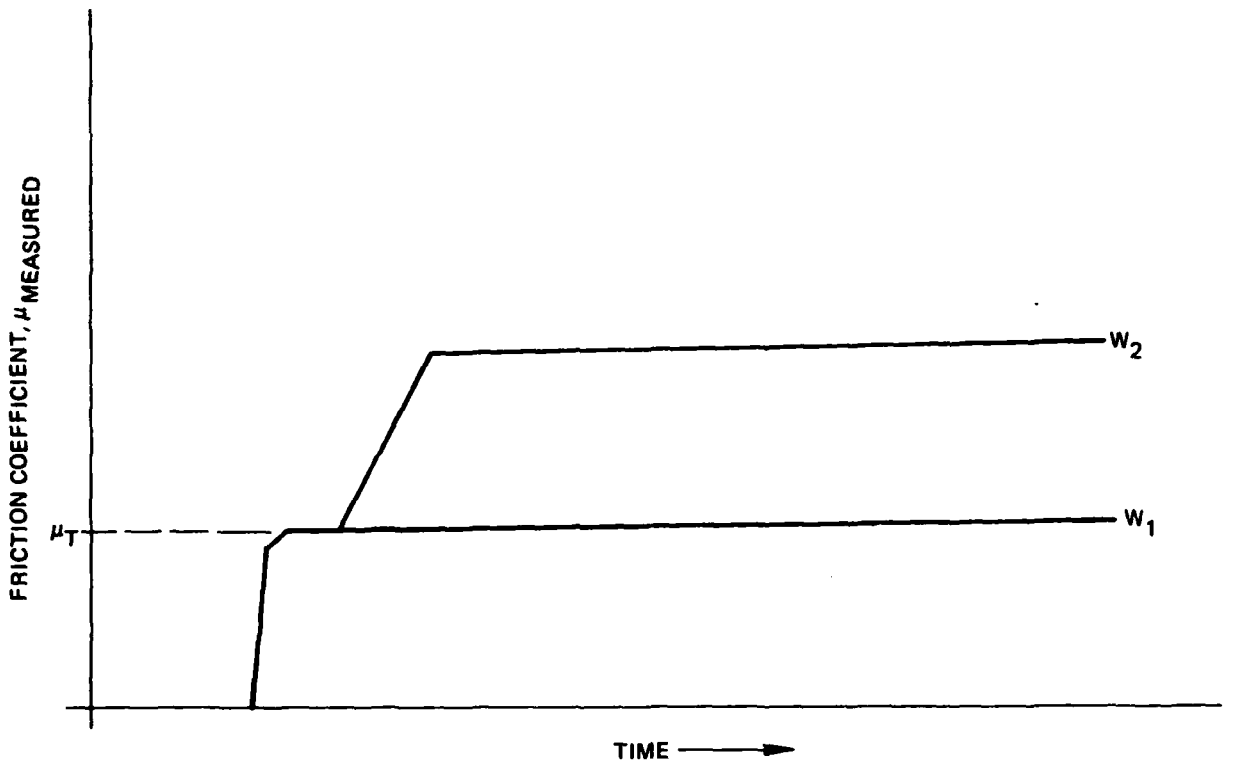

Figure 17. Schematic sketch showing effect of increases in applied load on friction trace characteristics of implanted Beryllium. $W_1 < W_2$ μ_T = true value of the friction coefficient. $\mu_{measured} = \mu_T + \mu_W$; where μ_W is dependent on wear of surface.

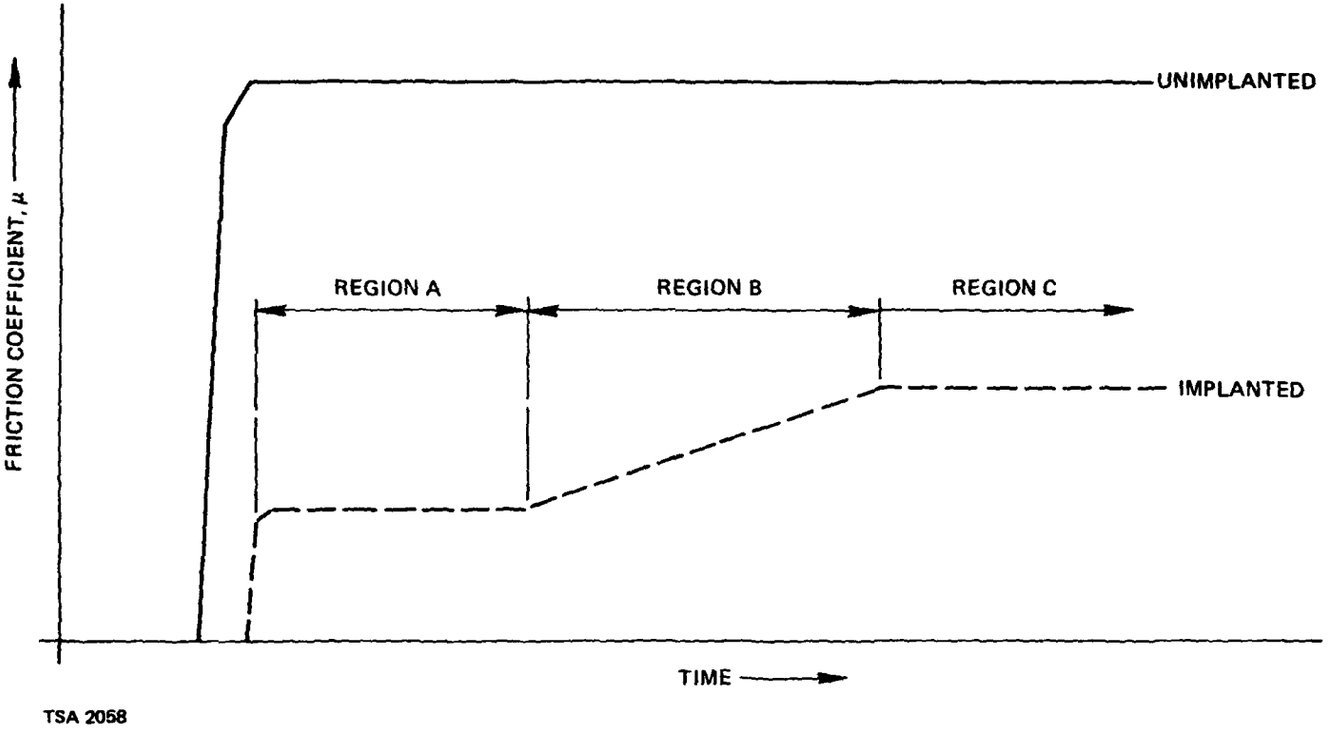

Figure 18. Schematic sketch of observed friction traces on unimplanted and implanted Beryllium. 1/8-inch ϕ sapphire ball used as pin.
Region A: No measurable wear; friction coefficient (μ) constant.
Region B: Gradually increasing wear of implanted region; μ increases rapidly.
Region C: Steady state wear; μ only increases very slowly.

For both the flat and the graded boron distributions, no material removal was observed at the 20-gm load. While the flat distribution samples had no observable wear track at 20 gm, there was a track visible on the graded sample. The wear data for loads greater than 20 gm indicated that the samples with the flat distributions are able to withstand higher loads before the onset of catastrophic wear. The graded sample was able to withstand a 40-gm load without failing whereas the flat boron distribution withstood a 50-gm load with little wear and 60 gm was required to produce substantial material removal.

All of these observations are indicated in Figures 19 and 20, which contain results both from an optical examination of the wear tracks obtained in samples NRL 40-V and NRL 40-VI, and from a surface profile examination using the Dektak. Figure 21 contains the surface profile obtained across the wear track in an unimplanted beryllium sample at a 20-g load for comparison. It is clear from all of this data that the flat profile samples are capable of withstanding greater loads before catastrophic wear occurs than are the graded layer samples for the same peak surface boron concentration. What was considered significant, however, was the lower values of the friction coefficient indicated on the flat profile samples compared to the graded profile samples.

It may be concluded from these measurements that the friction behavior of a sample surface (as indicated by the measured value of the coefficient of friction) is not determined only by the condition of the surface but is also influenced by what exists in the subsurface regions. It should be noted that the peak boron surface concentrations were near identical for both the flat and graded profile samples and the differences that existed were essentially confined to the subsurface regions.

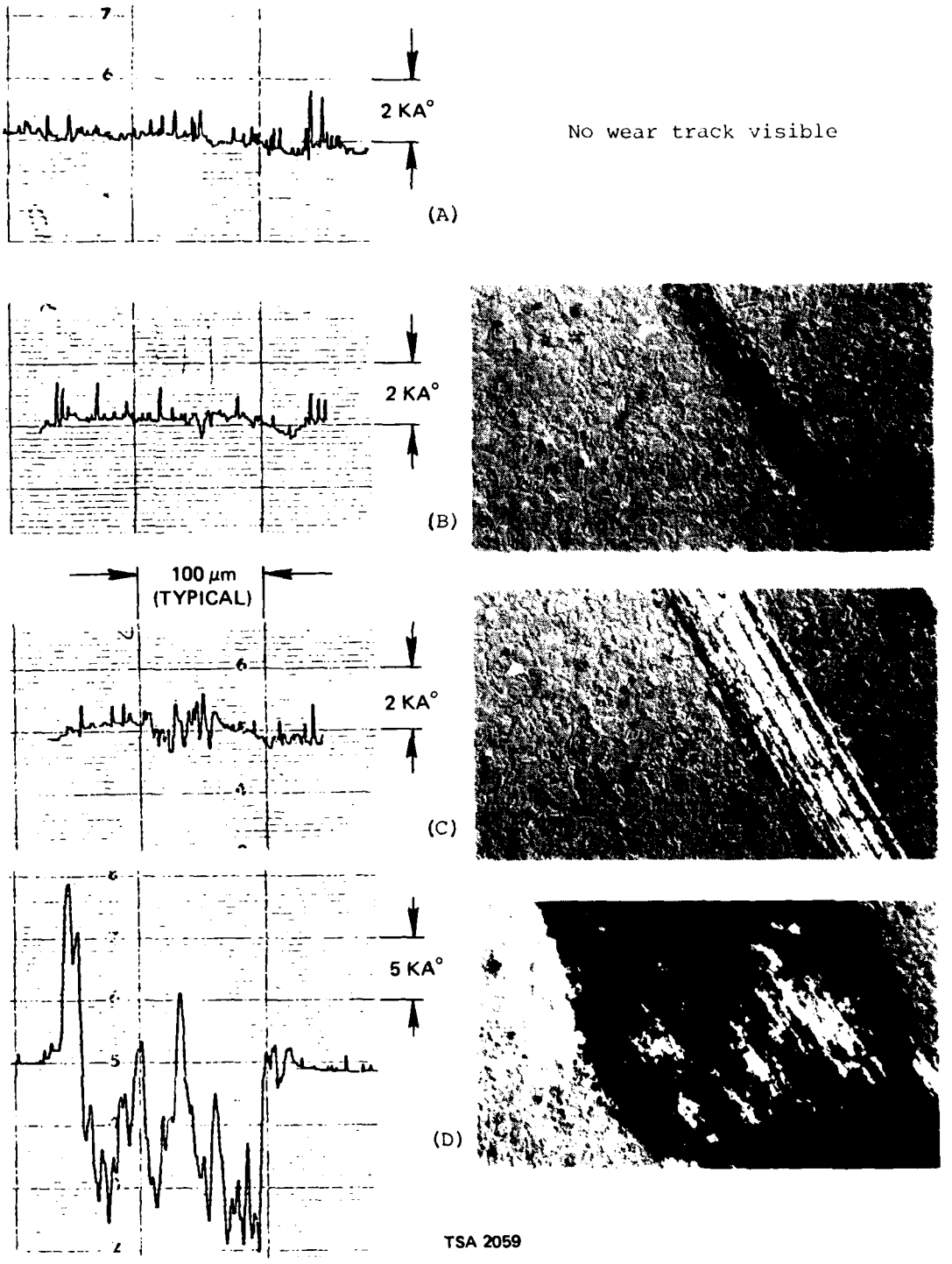

Figure 19. Sample 40-V. Surface profiles and accompanying micrographs of wear tracks made at different loads. (A) 30 g, (B) 40 g, (C) 50 g, (D) 60 g. Run time = 10 minutes at each load.

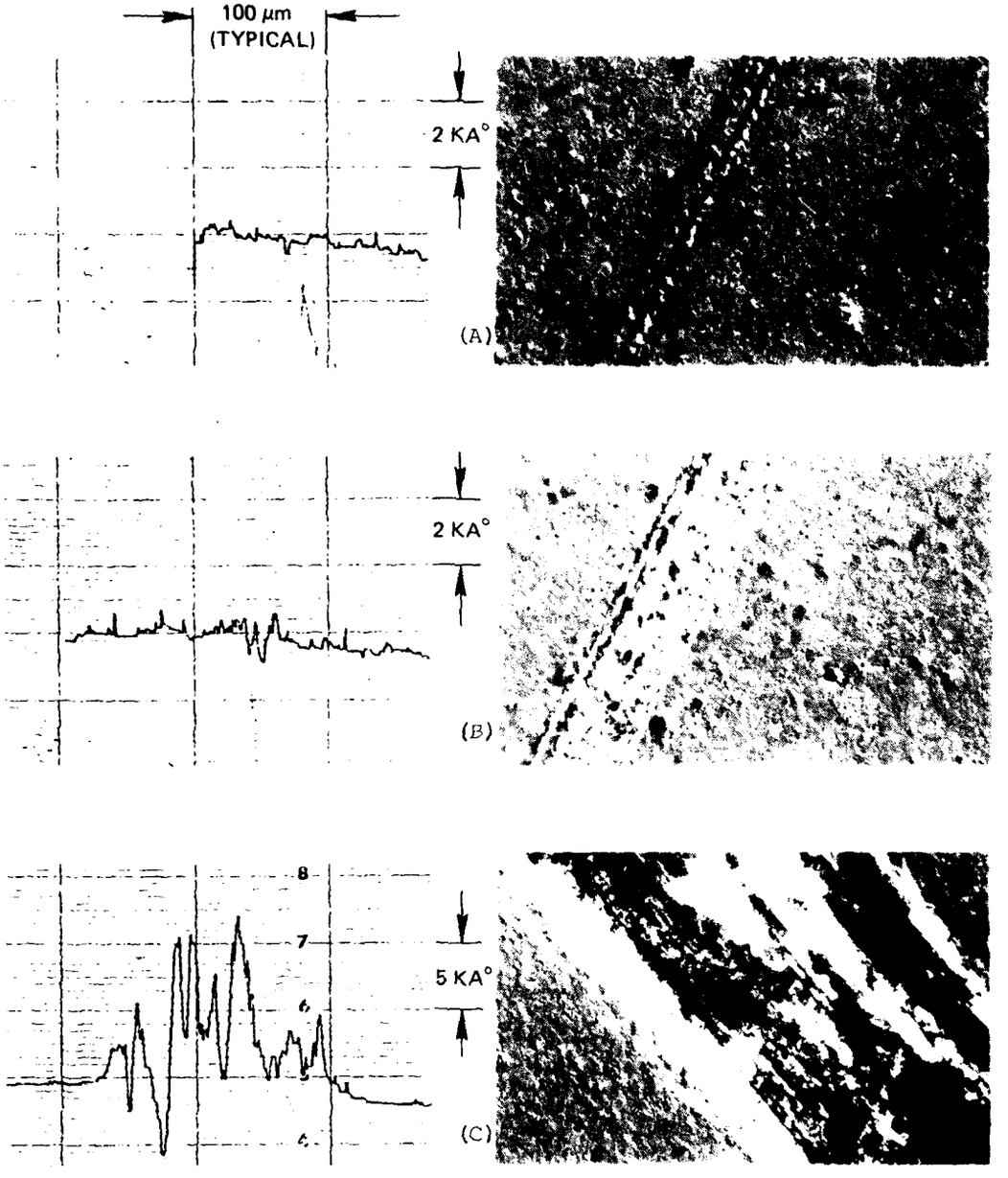

Figure 20. Sample 40-VI. Surface profiles and accompanying micrographs of wear tracks made at different loads. (A) 30 g, (B) 40 g, (C) 50 g.

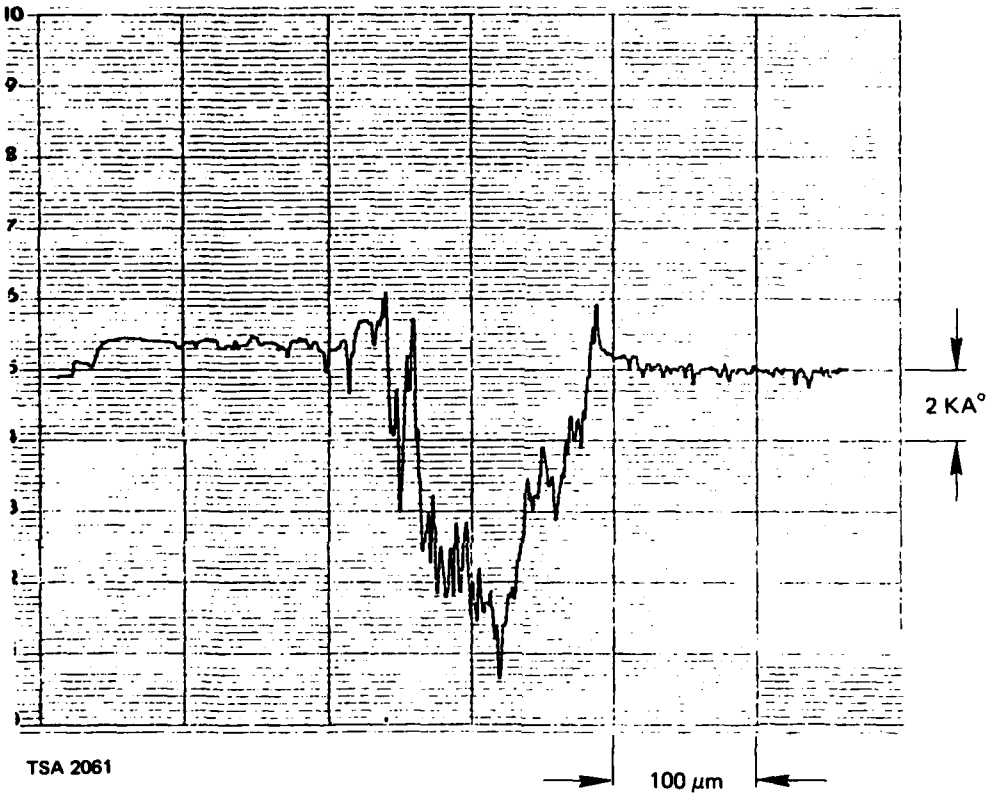

Figure 21. Unimplanted beryllium. Surface profile of wear track made at 20-g load. Time of test = 10 minutes.

The wear results obtained on these materials indicate that the graded profile samples (which also had a higher coefficient of friction) were also less wear-resistant than were the flat profile specimens. All of this would seem to indicate that the flat profile specimens are preferable to the graded profile materials from both the friction as well as the wear points of view.

SECTION 5

COMPOSITE MATERIAL

5.1 Introduction

Beryllium-ceramic metal matrix composites fabricated by hot isostatic pressing of blended powders are being examined as an alternate approach to the fabrication of hard, wear-resisting surfaces for use in gas bearings. Beryllium has served as the metal matrix principally because of its very desirable bulk properties. The physical properties of a composite made from this metal are, therefore, expected to be much more compatible to the rest of the gyro structural members than those either of a solid ceramic or of a composite fabricated using other metal constituents as the host material. It is anticipated that the physical characteristics of such composites will be between those of ceramic and beryllium. The benefits in using this type of composite lie in the recognition that the entire wear and friction process is confined to the ceramic particles standing out in relief at the surface of the composite.

5.2 Previous Work

5.2.1 Material Selection

The criteria that were used to select ceramic powders for fabricating these composites included the following:

(1) Microhardness

(2) Chemical stability

(3) Thermal expansion compatibility

A ceramic with a high value of microhardness was desired principally because hard materials are known to be resistant to degradation from processes such as impact and erosion and also because these display relatively low values of the coefficient of friction.[15] A low friction coefficient value is of interest because it permits the operation of the gas bearing at low starting torque levels. Evidence obtained on metal-ceramic composites has also indicated that composites which have high average values of microhardness are also more resistant to abrasive wear.[16] (Average microhardness of the composite is defined as the summation of the contributions of the microhardness values calculated in proportion to their respective value fractions within the composite.)

Chemical stability, which is indicated by the values of the free energies of formation of the several compounds, is of particular concern at the high temperatures that are used for hot consolidation of the metal-ceramic powders. While it is important that the metal matrix wet the ceramic, one does not want the metal to chemically reduce the ceramic at the temperature used for densification.

Thermal expansion compatibility consideration involves selecting a ceramic with an expansion coefficient only slightly lower than that of the surrounding metal resulting in a mild compressive state of stress around the particle. An expansion coefficient higher than the metal will cause the ceramic particles to pull away from the metal during cooling after hot consolidation whereas one considerably lower will result in a very high level of stress.

5.2.2 HIP Process Development

Beryllium-titanium diboride composite material fabricated during initial experiments at CSDL using the hot isostatic pressing technique demonstrated that the fabrication sequence in itself needed a certain amount of development effort. Poor densification was obtained in a sample that was isostatically densified at 900°C and 15 klb/in^2 gas pressure for 2 hours. Large pockets containing loose TiB_2 powder (which was the chosen ceramic) were observed with the unaided eye.

This problem was substantially corrected by resorting to high-energy powder blending (in a ball mill), outgassing of the powders at 600°C prior to container encapsulation, and using a higher densification temperature of 950°C.

5.2.3 Composite Development

Based on the selection criteria outlined above, the ceramics Al_2O_3, TiC and TiB_2 were chosen for further examination. Beryllium powder designated as -325 mesh was blended with powders of these different ceramics using the high energy blending procedure discussed above. The variations that were attempted pertained to type, percent volume, and particle size of the ceramic. The blended powders were cold pressed and subsequently hot isostatically pressed at 975°C for 4 hours under an inert gas pressure of 15 klb/in^2. An acid dissolution technique that vigorously attacked the steel cans (with little or no effect on the composite) was successfully employed for removal of the HIPed composite material.

Density measurements on these samples using the wet displacement technique showed that two of the 12 mixtures that were attempted achieved theoretical densities. In each of the four composites containing TiC, the values of density measured were considerably less than what was observed for the other mixtures, suggesting that the problems were probably related to insufficient outgassing of the TiC powders. This view was separately supported in that samples produced from coarse (-325-mesh) ceramic powders showed a higher level of densification than did similar samples made from the fine (1- to 2-micrometer) ceramic powders.

Lapping studies performed on coarse TiB_2-containing composites showed that use of coarse (500-grit-size) particle Al_2O_3 as the polishing compound resulted in the ceramic particles standing out considerably in relief above the beryllium surface. Scanning Electron Microscopy (SEM) observations showed that the surface of the recessed

beryllium after polishing with coarse particles was also quite rough after this polishing procedure. When this sample was subsequently polished with the finer Al_2O_3 pastes (the finest contained a 2- to 3-micrometer Al_2O_3 particle size), micromachining of the TiB_2 particles was observed. The recessed beryllium also had a smoother surface in these instances.

One of the more noteworthy observations made in this study was related to ceramic particle distribution in the composite. These observations indicated that the -325-mesh TiB_2 particle-containing composites were more desirable than were the 1- to 2-micron-containing composites. While the -325-mesh samples showed a reasonably uniform distribution of the particles throughout the beryllium matrix, the 1- to 2-micron samples showed that the ceramic particles were mainly segregated at the grain boundaries of the beryllium. Also, the 1- to 2-micron ceramic particles were not completely surrounded by the beryllium as compared to the -325-mesh particles, which showed an intimate physical contact betwen the ceramic and the beryllium (all around the ceramic particle). Micromachining effects of the ceramic particles were not observed in the 1- to 2-micron samples, possibly because of their very small particle size, and maybe even because of a lowered tendency of the particles to remain bonded to the matrix.

Another significant observation made during these investigations was the near absence of micromachining of the ceramic particles in the Al_2O_3 containing 5545-0 composite. The SEM observations on the as-lapped condition of this composite showed the existence of reasonably large voids in sizes comparable to the -325-mesh Al_2O_3 particles. The view that these voids resulted from Al_2O_3 particle pull-out during the several lapping operations that the composite was subjected to during disc sample preparation was directly supported by microstructure observation which showed that void shape was similar to particle shape, and by a density measurement using the wet displacement technique, which showed that the as-pressed density of this material was close to what was theoretically considered the maximum. Furthermore, any voids formed

at the HIP temperatures, due to inadequate sinte ng, were expected to be close to spherical in shape and not possess the irregular features that were obse. ved for this sample.

All of these observations indicated extremely poor bonding of the Al_2O_3 particles to the beryllium matrix. It was concluded that further research efforts should be directed at developing only the TiB_2-containing composite materials. All of this work was discussed in much greater detail in References 11 and 17.

5.3 Present Work

5.3.1 Surface Preparation

All of the sample surface preparation discussed in the last reporting period[11] was limited to lapping these composites using polishing compounds which contained differently sized Al_2O_3 powder particles as the hard abrasive medium. This procedure, however, took an inordinately long time for preparing the samples. It also resulted in sample surfaces which had a matte appearance accentuated by the ceramic particles standing out in relief above the polished beryllium surface. Sample preparation using polishing compounds containing diamond particles was, therefore, investigated on these materials. This polishing was performed using hand-held procedures (unlike the work with the Al_2O_3-containing compounds in which a Crane Lapmaster machine was used) with the hope that good, shiny surfaces could be generated in a shorter period of time.

Figure 22 was obtained on a 4545B composite sample and is typical of what can be achieved using diamond as the the lapping medium. The scheme used for sample nomenclature was discussed in Reference 11. 4545B corresponds to a composite containing 45 volume percent of TiB_2 with ceramic particle sizes less than 45 μm (-325 mesh). The ceramic particles appear as severely pitted by the action of the diamond particles. Fine scratches are also observed on the softer beryllium matrix.

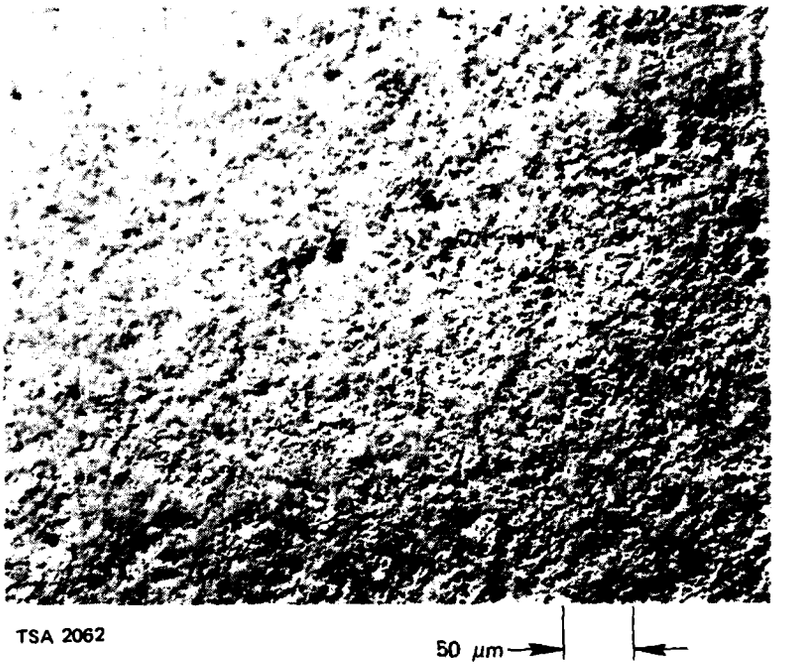

Figure 22. As-lapped diamond surface. Sample 4545B.

This micrograph and the others presented in this section of this report were all obtained using differential phase contrast (Nomarski) microscopy to highlight the extent of the differences that exist in the height levels of the TiB_2 particles with respect to the surrounding matrix. Little height differences are noted in this micrograph which was obtained after lapping the 4545B sample on an 1800-grit-size Abernathy Lap following an earlier lapping treatment sequence on 600-grit-size SiC paper and 600-grit-size Abernathy lap. (Abernathy laps are commercially procured and consist of a diamond particle dispersion in an alumina matrix.)

Figure 23 contains a series of micrographs obtained on the 4545B sample at various stages of polishing showing the gradual removal of ceramic particle damage introduced by the diamond particles embedded in the Abernathy lap. The micrographs shown as Figures 23(B) and 23(C) show that although polishing the sample with fine particle (0.05-μm) Al_2O_3 did gradually remove the damage observed after a 10 minute lapping operation on a 600 grit size Abernathy Lap followed by 2 minutes lapping on cloth using Syton, which is a commercially available ultra-fine particle SiO_2 suspension, it did so in addition to producing considerable relief of the ceramic particles at the surface. (It is interesting to note in Figure 24 that an additional lapping of the Al_2O_3 polished specimen with a 0.25-μm diamond again resulted in damage to the ceramic particles.)

In contrast to these observations, the micrographs in Figure 25 show damage removal at the sample surface in a 10-minute, 1800-grit-size Abernathy lap processed specimen using only Syton as the polishing medium. In this case, the microstructure appears to be characterized by a somewhat lesser relief as indicated in these Nomarski micrographs. It appears that Syton is a better polishing medium for these materials (following earlier polishing treatments with progressively finer diamond). The lesser indicated ceramic particle relief from the Syton is suspected to have resulted from the much finer particle size of the SiO_2 in suspension (in Syton) as compared to the 0.05-μm Al_2O_3.

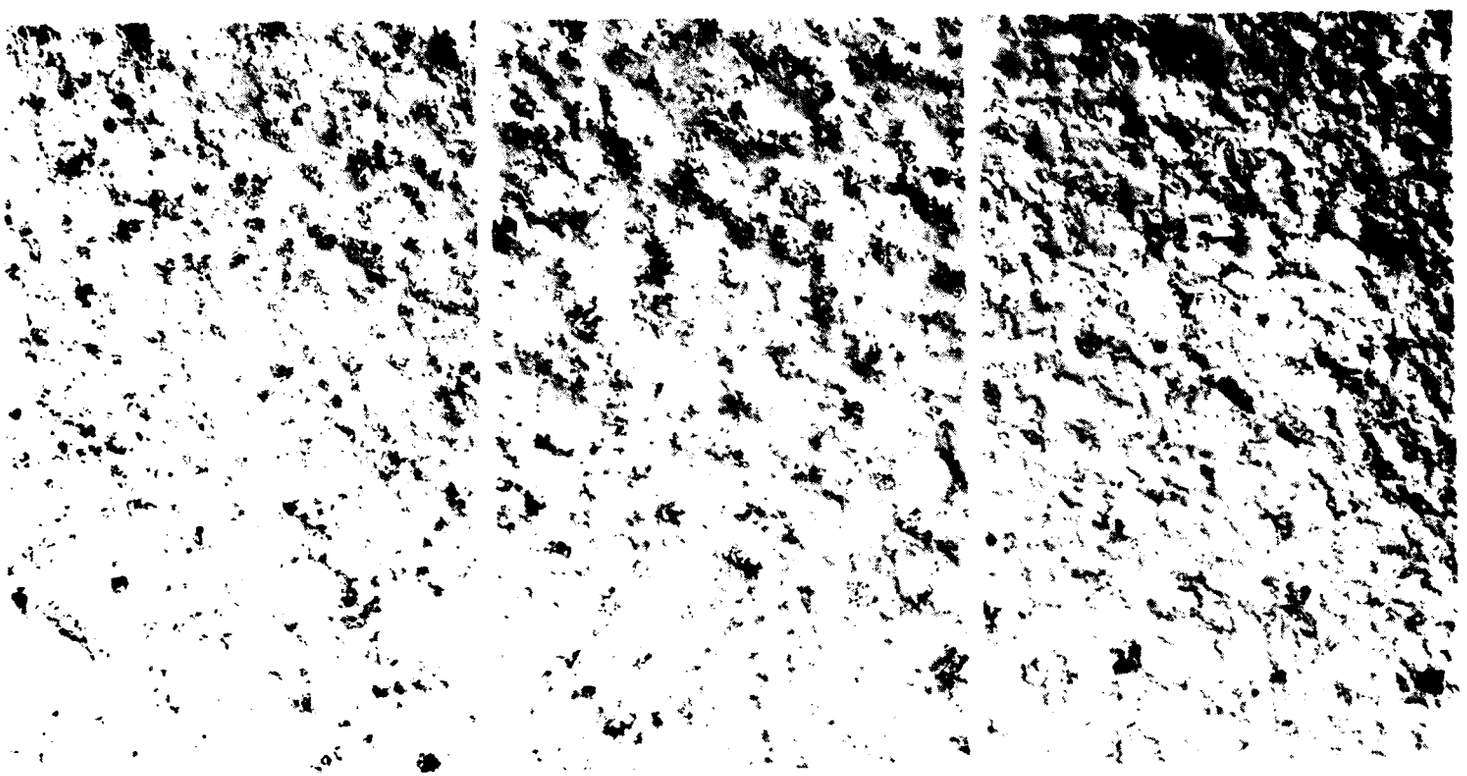

TSA 2063

Figure 23. Different stages of lapping of 4545B sample. (A) As lapped 600 grit, diamond + 2 minutes Syton. (B) (A) + 2 minutes with 0.05μm Al_2O_3. (C) (B) + 2 minutes additional with 0.05μm Al_2O_3.

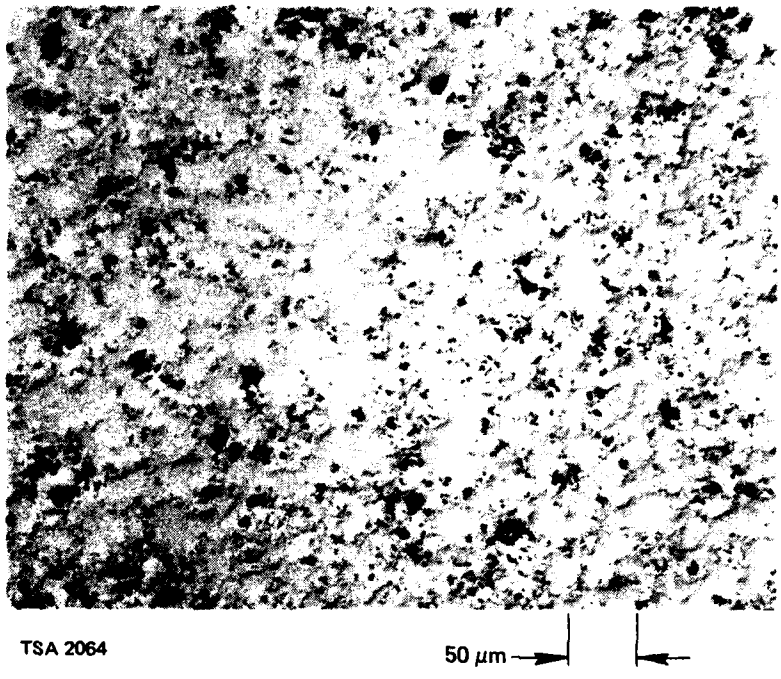

Figure 24. 4545B surface after 5 minutes polishing with 0.25-μm diamond following sequence in Figure 23(C).

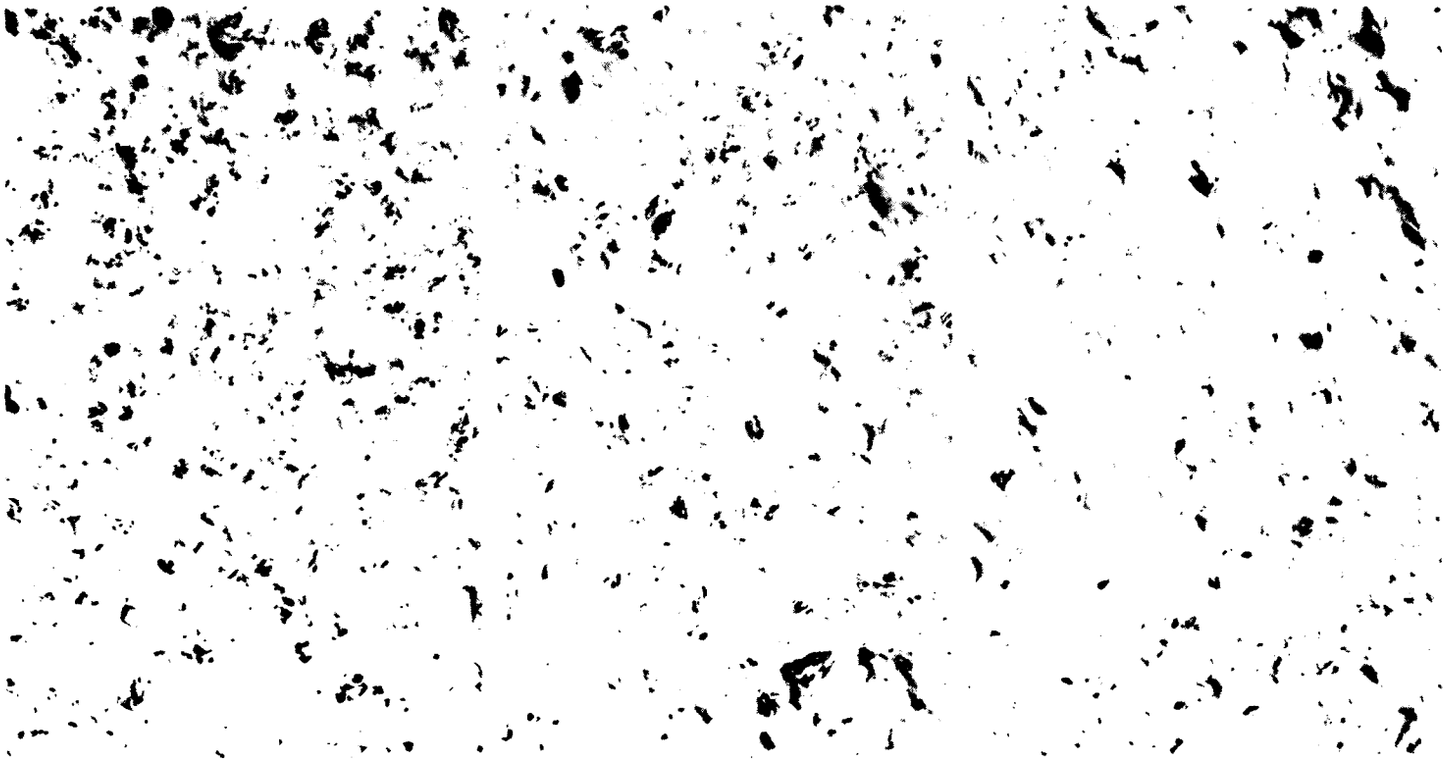

Figure 25. Polishing observed on sample after different stages.
(A) 10 minutes 1800 grit diamond + 1 minute Syton.
(B) (A) + 1 minute Syton. (C) (B) + 1 minute Syton.

5.3.2 Friction and Wear Testing

All of the wear testing reported in this section was performed on the compositions containing TiB_2 as the ceramic. Initial wear testing of these materials consisted of performing high speed (about 200 r/min) rubbing experiments between the flat surfaces of disc-shaped samples in a disc-on-disc format. This procedure of testing was discarded when it was recognized that establishing a surface-to-surface contact during testing was nearly impossible to attain in that the samples were invariably cocked in the running position. This made a reliable measurement of the coefficient of friction impossible to attain with any degree of confidence.

In each instance, it was noted from the scoring of the surfaces that contact between the surfaces of the two mating discs was only established in a few discrete locations. A pin-on-disc format for wear testing was, therefore, subsequently examined. The pin selected for testing purposes was cored from a disc of the 3545B composite using electrical discharge machining (EDM). The surface of this pin was flat because difficulties were encountered in the machining of these materials making it very time consuming to establish a curvature at the tip of the pin. The differences between the wear test using a flat pin and a conventional test which uses a pin with a curvature at the bottom is shown schematically in Figure 26. Cocking problems persisted, resulting in dragging of the edge of the cylindrical pin on the composite surface. This resulted in some transfer of the beryllium in the pin onto the sample surface.

The buildup of material on the sample surface resulting from these experiments is shown in Figure 27, which contains two Dektak surface profiles of the wear tracks on the sample surface. SEM photographs taken on these specimens at high magnification (Figure 28) show a scored sample surface (resulting from dragging and wearing of the edge of the pin) and what appears as an untouched pin surface following the wear testing.

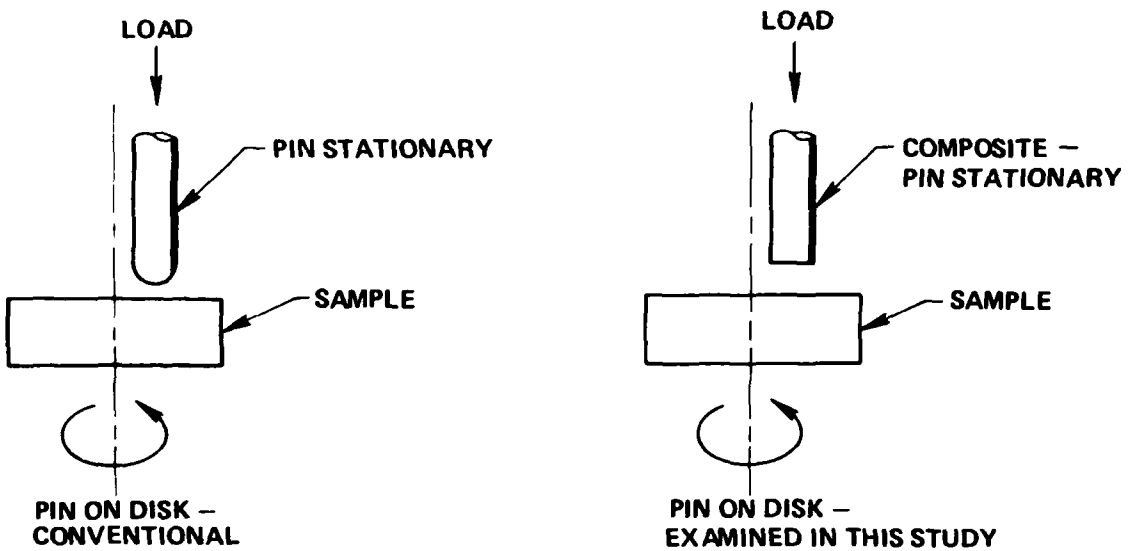

Figure 26. Wear testing procedures - schematic.

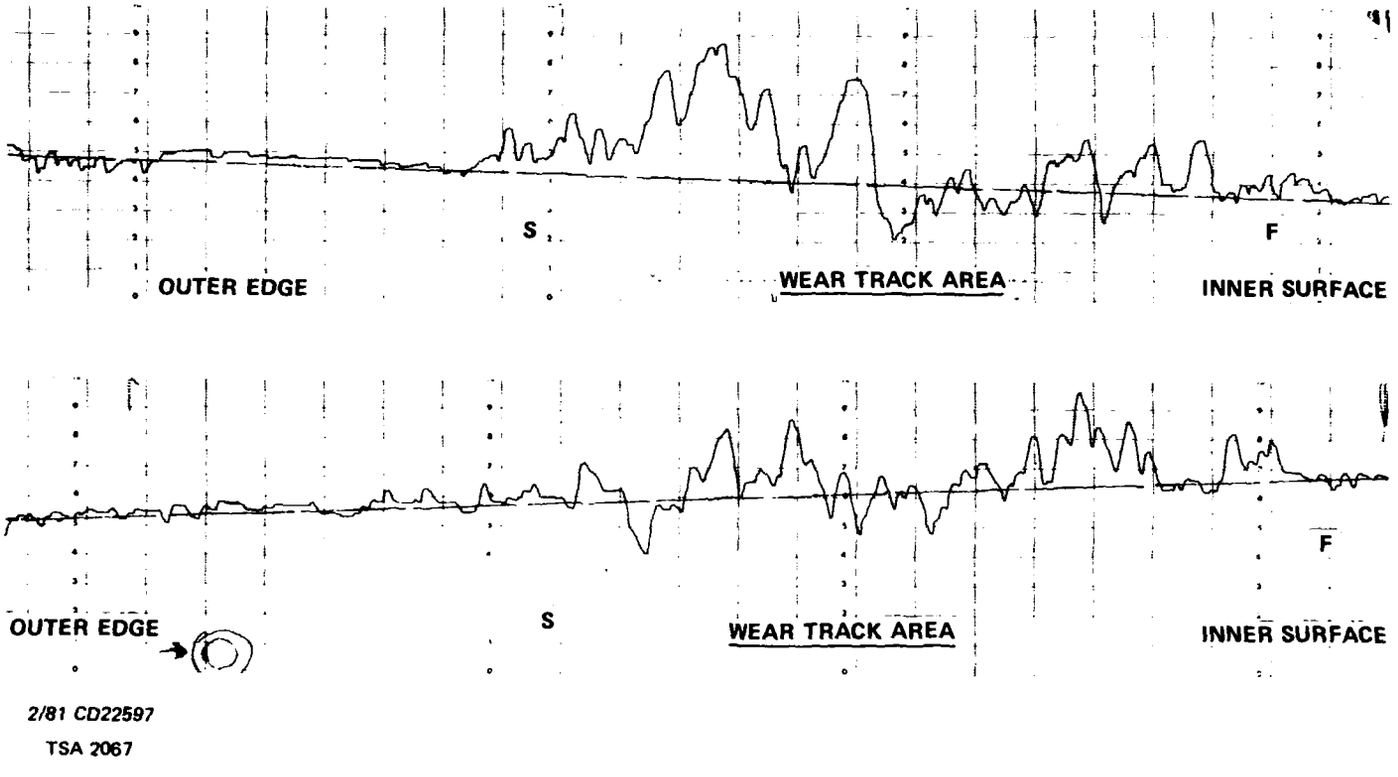

Figure 27. Dektak profiles of wear track in 3545B.

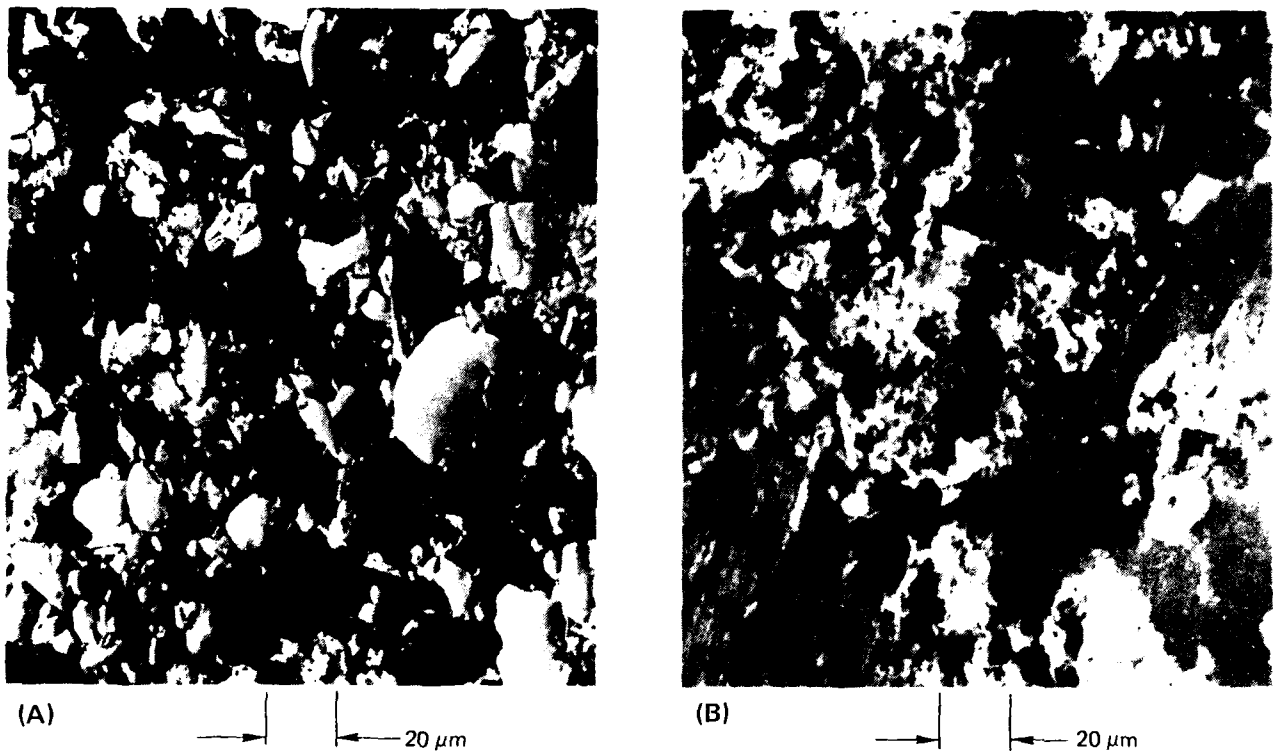

4/81 CD23442
TSA 2068

Figure 3%. Results of initial wear experiment.
(A) Surface of pin. (B) Surface of disc sample.

It was not possible to examine the edge of the pin from where material removal was suspected to have occurred because of effects of charging. Since the friction data was suspect even in this case, it was finally decided to examine ways of placing a curvature at the end of a cylindrical composite pin. This was finally achieved and additional testing is tentatively planned with this pin.

In the interim, friction and wear testing was also attempted using a sapphire pin. This pin was constructed using suitably sized sapphire balls, commercially available, rigidly held in a fixture that was designed for this purpose. Initial runs were performed with a 1/8-inch diameter sapphire ball at an applied load of 30 gm and a linear speed of roughly 80 to 95 mm per second. Substantial build-up of debris was observed on the sample surface and considerable wear of the sapphire ball was noted in each instance.

To more closely approach a disc-on-disc type of evaluation and to minimize the effect of surface grinding (or plowing) of the sapphire ball by protruding TiB_2 particles it was decided to perform additional tests with larger sized sapphire balls. The additional ball diameters investigated were 1/4-inch and 3/8-inch. In each instance, however, severe wear was observed on the ball surface with an accompanying build-up of material on the sample surface.

All of the observations made are shown in Figures 29 and 30. The wear on the ball was observed optically and build-up of material on the sample surface was examined using a Dektak surface profilometer. The friction data obtained from these experiments are listed in Table 11. This table also contains data on similar experiments performed on an identically produced sample surface which was etched for 15 seconds for preferential beryllium dissolution, prior to the wear test experiments.

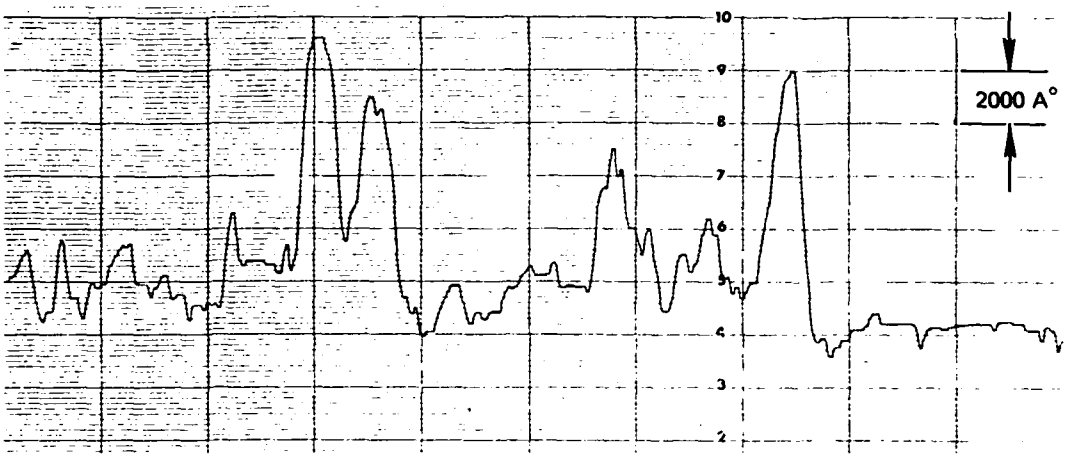

(A) 1/4 inch diameter ball.

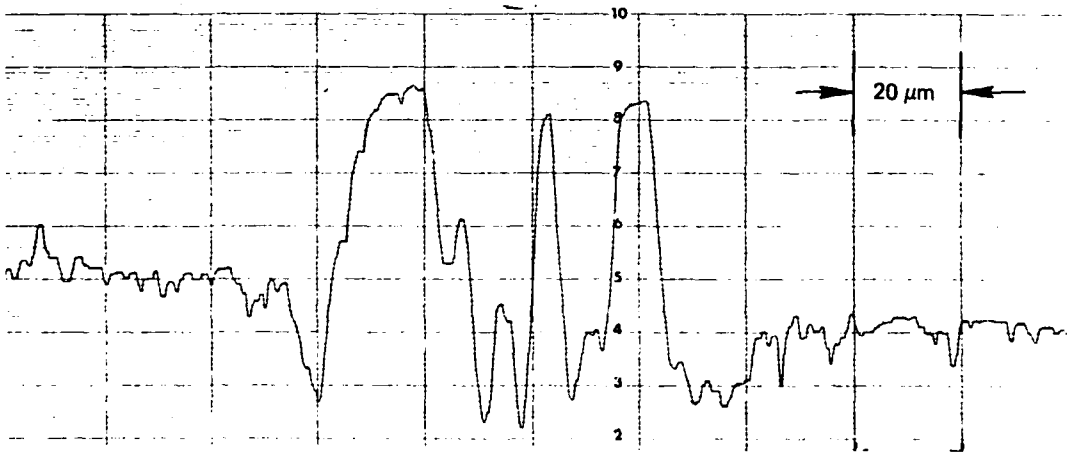

(B) 3/8 inch diameter ball.

TSA 2069

Figure 29. Wear track profiles across 4045B sample.

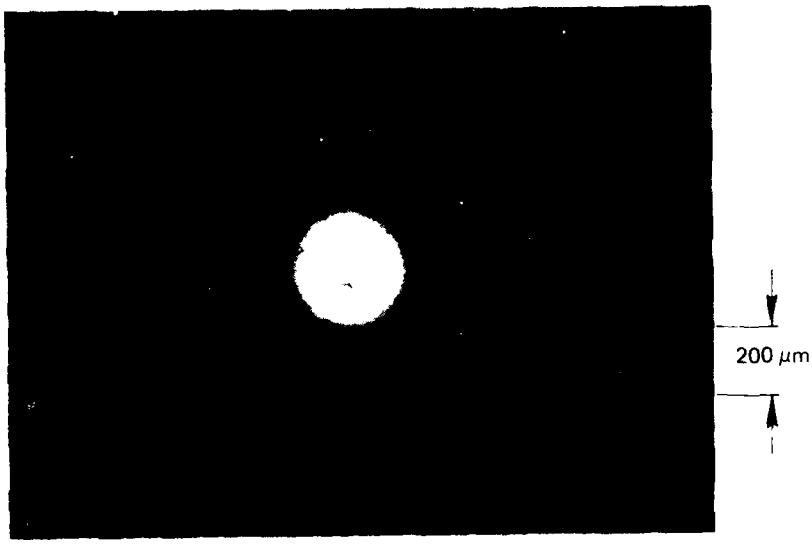

(A) 1/4 inch diameter ball

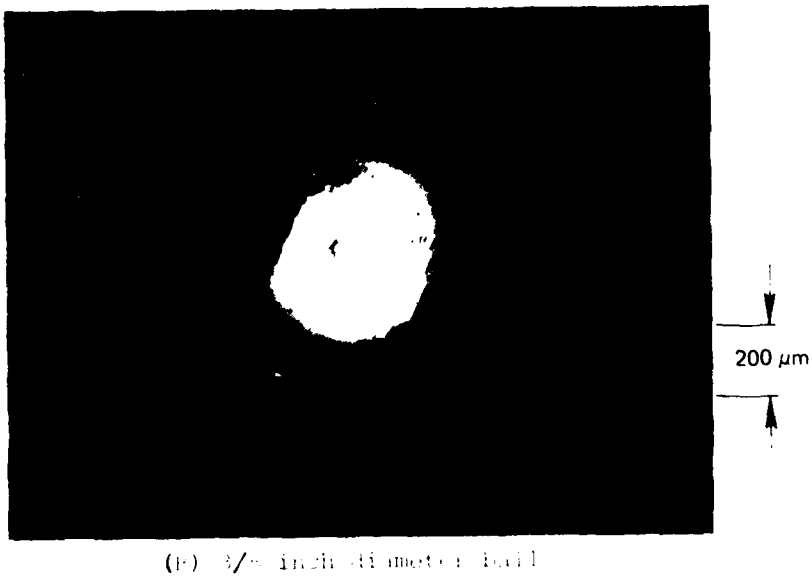

(B) 3/8 inch diameter ball

TSA 2070

Figure 30. Wear [illegible]

Table 11. Friction data obtained with differently sized sapphire balls on sample 4045B.

Sample Condition	Load (g)	Ball Size (inch)	Time of Run (minutes)	Friction Coefficient (μ)
As-lapped	30	1/8	30	.26
As-lapped	30	1/4	30	.50
As-lapped	30	3/8	30	.29
After 5-sec etch	30	1/8	30	.39
After 5-sec etch	30	1/4	30	.41
After 5-sec etch	30	3/8	30	.23

Observations made of the etched composite sample after the wear runs indicated that these were qualitatively similar to what was observed for the as-lapped condition. Wear of the sapphire ball essentially resulted from contact with the TiB_2 particles and the beryllium matrix had little or no role in influencing the wear of the sapphire balls against the 4045B composite specimen. The only apparent differences that were observed between the two samples were related to the surface profiles which showed that the etched specimen had a much rougher sample surface due to the preferential etching of the beryllium with the etching solution.

5.3.3 Measurement of Thermal Expansion

Th coefficient of thermal expansion was measured for three different TiB_2-containing composite compositions. These corresponded to composites with 35, 40 and 45 volume percent TiB_2 in a particle size designated as -325 mesh (or, less than 45 μm). The temperature range over which the measurements were made was 40 to 90°C.

Briefly, the technique consisted of determining the thermal expansion of the several materials with respect to temperature using bonded resistance strain gages. The dilation of the test materials was determined versus National Bureau of Standards (NBS) Reference Material

736 (copper) by the resistance gages of known characteristics. In this experiment, a sample of instrument grade I-400 beryllium was also included as a further check on the measured values. The specimens were heated by means of a stirred, temperature-controlled oil bath. The bath temperature was determined with an NBS-calibrated mercury-in-glass thermometer. The values of the expansion coefficients were determined from the measured data by calculating the slope of the chord connecting the end points of the expansion curve.

The values that were measured for the several samples are shown in Table 12. The values for the composite materials were lower than expected initially on the basis of the volume percent of the ceramic and the published value of 4.8×10^{-6} per °F for TiB_2.[18] It would appear that in the low temperature region, which is of interest to inertial instrument designers, the expansion coefficient of TiB_2 is substantially smaller than the published value.

Table 12. Measured values of the coefficient of thermal expansion $\alpha(\times 10^{-6})$.

Sample	Vol % Ceramic	$\alpha(10^{-6})$	
		Per °F	per °C
3545B	35	5.0	8.9
4045B	40	4.8	8.7
4545B	45	4.7	8.5
I-400 beryllium	0	6.7	12.1

5.3.4 Fabrication of Composites with Narrowly Sized TiB_2 Powders

Earlier work with samples made from coarse (-325-mesh) and fine (1- to 2-μm) TiB_2 powders had indicated a need for evaluating composite integrity using narrowly sized TiB_2 powders for composite fabrication. Because conventional sizing procedures using differently sized sieves would not have yielded size classifications below about 450 mesh (35 μm), it was decided to use the alternate procedure of air classification instead.

The air classification was performed on an Alpine American Corporation 100 MZR unit and size ranges corresponding to -10, -20 +10, -30 +20 and +30 μm were obtained. (A minus sign indicates particles less than the following size in μm and a plus sign indicates particles greater than the stated size. For example, a -20 +10 μm size fraction implies that the particles are greater than 10 μm , but smaller than 20 μm). The size fractions that were obtained from about 4.2 lbs of commercially procured -325-mesh TiB_2 powder are shown in Table 13.

Table 13. Amount of powder collected for different size ranges.

Size Fraction (μm)	Amount Collected (g)	% of Total Amount
-10	1.06	25.4
-20 +10	1.99	47.6
-30 +20	0.66	15.8
+30	0.47	11.2

These classified powders were subsequently blended with -325-mesh beryllium powder (using techniques that were developed earlier) to give identical compositions of 45 volume percent ceramic, cold isostatically pressed in rubber boots, encased in low carbon steel cans and HIPed at 1000°C and 30 kpsi argon gas pressure. Samples obtained from these

different compositions will be evaluated for friction and wear to determine optimal particle size range for the ceramic. It is unfortunate that similarly sized beryllium powder cannot be obtained commercially, principally because it is difficult to handle beryllium owing to its toxicity and also because the different beryllium size ranges will contain different levels of beryllium oxide which would represent an additional variable (aside from the different TiB_2 particle size range) in the overall experimentation.

5.3.5 Fabrication of Near-Net Shape Parts

Because of the many difficulties that are encountered in the machining of these materials using conventional procedures, it is important to be able to fabricate parts of this composite in near-net shape and size. The design that has been examined is that of a cylindrical geometry with a hole running across the axis and this forms part of a spool type gas bearing.

Our initial experiment in this regard dealt with cold isostatically pressing the required blend of powders (TiB_2 and beryllium) around a pre-machined 430 stainless steel mandrel shaped in the form of several ribbed sections, as shown in Figure 31, to yield several parts in close-to-finished size. Figure 32 shows an isostatically pressed specimen which was enclosed in a low carbon steel can following cold pressing and subsequent HIPed at 1000°C and 30 kpsi gas pressure. 430 stainless was selected primarily because of its greater thermal expansion match to beryllium and because it does not undergo the structural (and associated discontinuous dimensional) change at about 760°C that low carbon steels are characterized by during heating and cooling cycles which include excursions through this eutectoid temperature.

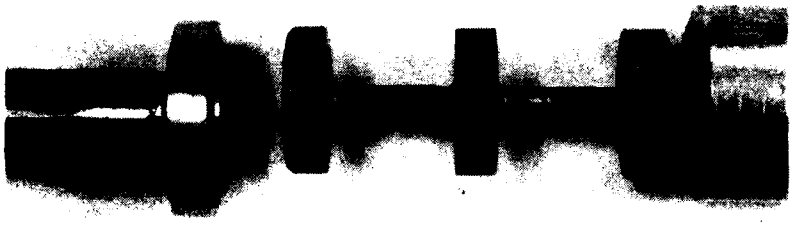

TSA 2071

Figure 31. Ribbed 430 stainless mandrel. Also observed are low C steel parts of the cannister in which HIPing was performed subsequent to cold pressing of blended powder around the mandrel.

TSA 2072

Figure 32. View of near-net shape parts HIPed around 430 stainless mandrel.

A disadvantage of using this material, however, is that unlike low carbon steel which can be dissolved readily in a warm 50 percent solution of nitric acid, the 430 stainless will have to be machined. This makes the process more expensive than desired, even though the expenses incurred are still significantly lower than what are typically associated with conventional machining of these composites and therefore amount to substantial savings. Following examination of parts produced by this procedure, it is anticipated that additional experimentation will be attempted using low carbon steel mandrels.

5.3.6 Industrial Application of Processed Materials

Even though the efforts made so far at reliably evaluating the wear and friction characteristics of these materials have proved quite difficult, another evaluation (more pertinent from a gas bearing point of view) has nevertheless been performed on these composites. Based on the results obtained so far under this program, a -325 mesh TiB_2-containing composition was selected and HIPed using powder consolidation procedures initially investigated under CSDL funding and subsequently refined under the present contract.

An actual gas bearing, of the spool type was constructed with this material at a commercial vendor's facility under separate government sponsorship. Relevant tests were performed and no apparent visible degradation of the gas-bearing wheel was observed. These initial, very promising tests have served as the basis for a substantially more expanded wheel build and evaluation effort at the vendor's facility under a separately funded government program.

REFERENCES

1. Keating, W.H., Compliance Coefficient Test Results for TGG No. 222X, Component Development Department, Memorandum No. 30H-76-541, The Charles Stark Draper Laboratory, Inc., December 1976.

2. Kumar, K., Analysis of $W_{(x)}$ C Sputter Deposits, Report No. C-4749, The Charles Stark Draper Laboratory, Inc., October 1976.

3. Morkovsky, L. Ya, D. Kondraskev Yu, and G.V. Kaputovskaya, The Composition and Properties of Beryllium Borides, J. Gen. Chem. U.S.S.R., Vol. 25, 1955, p. 1007.

4. Tupitsyn, I.I., I.I. Lyakhavskaya, M.S. Nakhmanson, and A.S. Sukhik, Energy Structure of Beryllium Diboride, Sov. Phys. Sol. State, Vol. 16, No. 16, April 1975.

5. Hoenig, C.L., C.F. Cline, and D.E. Sands, Investigation of the System Beryllium-Boron, J. Am. Ceram. Soc., Vol. 44, No. 8, p. 385, August 1961, p. 385.

6. Laubengayer, A.W., D.T. Hurd, A.E. Newkirk, and J.L. Hoard, Preparation and Properties of Pure Crystalline Boron, J. Am. Chem. Soc., Vol. 65, 1943, p. 1924.

7. Croft, W.J., N.C. Tombs, and J.F. Fitzgerald, Preparation and Characterization of Boron Films from Diborane, Mat. Res. Bull., Vol. 5, 1970, p. 489.

8. Das, D., and K. Kumar, Chemical Vapor Deposition of Boron on a Beryllium Surface, Thin Solid Films, 83, 1981, pp. 53-60.

9. Kumar, K., and D. Das, Structure Modification of β-Boron by Plasma Spraying, Met. Trans., Vol. 11A, 1980, p. 1489.

10. Koehler, K., "Flex Pivot Wear Tester--Design and Operation," CSDL Report No. C-5413, June 1981. ONR contract No. N00014-77-C-0388.

11. Das, D., K. Kumar, E. Wettstein, J. Wollam, Materials Research for Advanced Inertial Instruments, Task 2: Gas Bearing Material Development by Surface Modification of Beryllium, Technical Report R-1434, The Charles Stark Draper Laboratory, Inc., December 1980.

12. Kant, R.A., J.K. Hirvonen, A.R. Knudson, and J. Wollam, "Surface Hardening of Beryllium by Ion Implantation," Thin Solid Films, 63, 1979, p. 27.

13. Das, D., K. Kumar, E. Wettstein, J. Wollam, Materials Research for Advanced Inertial Instruments, Task 2: Gas Bearing Material Development by Surface Modification of Beryllium, Technical Report R-1330, The Charles Stark Draper Laboratory, Inc., October 1979.

14. Kant, R.A., K. Kumar, A. Knudson, "Mechanical and Microstructural Properties of Boron Implanted Beryllium," 1981 Annual Meeting of the Materials Research Society, Boston, Massachusetts 02139.

15. Rabinowicz, E., Friction and Wear of Materials, John Wiley and Sons, Inc., New York, 1965.

16. Ondracek, G., B. Leder, and C. Politis, Quantitive Metallography of Metal-Ceramic Composites, Prakt. Metallogr., 5 (2), 1968, pp. 71-84.

17. Kumar, K., D. Das, and K Koehler, "Beryllium-Ceramic Composites Using HIP for Gas Bearings," 1981 Annual Meeting of the American Ceramic Society, Washington D.C.

18. Engineering Properties of Selected Ceramic Materials, Battelle Memorial Institute, Columbus, Ohio, published by the American Ceramic Society, 1966.

BASIC DISTRIBUTION LIST

Organization	Copies
Defense Documentation Center Cameron Station Alexandria, VA 22314	12
Office of Naval Research Department of the Navy 800 N. Quincy Street Arlington, VA 22217	
ATTN: Code 471	1
Code 102	1
Code 470	1
Commanding Officer Office of Naval Research Building 114, Section D 666 Summer Street Boston, MA 02210	1
Commanding Officer Office of Naval Research Branch Office 536 South Clark Street Chicago, IL 60605	1
Office of Naval Research San Francisco Area Office 760 Market Street, Room 447 San Francisco, CA 94102	1
Naval Research Laboratory Washington, DC 20375	
ATTN: Code 6000	1
Code 6100	1
Code 6300	1
Code 6400	1
Code 2627	1
Naval Air Propulsion Test Center Trenton, NJ 08628	
ATTN: Library	1
Naval Construction Batallion Civil Engineering Laboratory Port Hueneme, CA 93043	
ATTN: Materials Division	1
Naval Electronics Laboratory San Diego, CA 92152	
ATTN: Electron Materials Science Division	1
Naval Missile Center Materials Consultant Code 3312-1 Point Mugu, CA 92041	1
Commanding Officer Naval Surface Weapons Center White Oak Laboratory Silver Spring, MD 20910	
ATTN: Library	1
David W. Taylor Naval Ship Research and Development Center Materials Department Annapolis, MD 21402	1
Naval Undersea Center San Diego, CA 92132	
ATTN: Library	1
Naval Underwater System Center Newport, RI 02840	
ATTN: Library	1

BASIC DISTRIBUTION LIST (Continued)

Organization	Copies
Naval Air Development Center Code 302 Warminster, PA 18964 ATTN: Mr. F.S. Williams	1
Naval Air Systems Command Washington, DC 20360 ATTN: Codes 52031 52032	1
Naval Sea System Command Washington, DC 20362 ATTN: Code 035	1
Naval Facilities Engineering Command Alexandria, VA 22331 ATTN: Code 03	1
Scientific Advisor Commandant of the Marine Corps Washington, DC 20380 ATTN: Code AX	1
Naval Ship Engineering Center Department of the Navy Washington, DC 20360 ATTN: Code 6101	1
Army Research Office P.O. Box 12211 Triangle Park, NC 27709 ATTN: Metallurgy and Ceramics Program	1
Metals and Ceramics Division Oak Ridge National Laboratory P.O. Box X Oak Ridge, TN 37380	

Organization	Copies
Naval Weapons Center China Lake, CA 93555 ATTN: Library	1
Naval Postgraduate School Monterey, CA 93940 ATTN: Mechanical Engineering Department	1
NASA Headquarters Washington, DC 20546 ATTN: Code RRM	1
NASA (216) 433-400 Lewis Research Center 21000 Brookpark Road Cleveland, OH 44135 ATTN: Library	1
National Bureau of Standards Washington, DC 20234 ATTN: Metallurgy Division Inorganic Materials Division	1
Director Applied Physics Laboratory University of Washington 1013 Northeast Fortieth Street Seattle, WA 98105	1
Defense Metals and Ceramics Information Center Battelle Memorial Institute 505 King Avenue Columbus, OH 43201	1

BASIC DISTRIBUTION LIST (Continued)

Organization	Copies
Army Materials and Mechanics Research Center Watertown, MA 02172 ATTN: Research Programs Office	1
Air Force Office of Scientific Research Building 410 Bolling Air Force Base Washington, DC 20332 ATTN: Chemical Science	1
Directorate Electronics and Solid State Sciences Directorate	1
Air Force Materials Laboratory Wright-Patterson AFB Dayton, OH 45433	1
Library Building 50, Room 134 Lawrence Radiation Laboratory Berkely, CA	1
Los Alamos Scientific Laboratory P.O. Box 1663 Los Alamos, NM 87544 ATTN: Report Librarian	1
Argonne National Laboratory Metallurgy Division P.O. Box 229 Lemont, IL 60439	1
Brookhaven National Laboratory Technical Information Division Upton, Long Island New York 11973 ATTN: Research Library	1
Office of Naval Research Branch Office 1030 East Green Street Pasadena, CA 91106	1

AD-A113 518 CHARLES STARK DRAPER LAB INC CAMBRIDGE MA F/G 13/9
MATERIALS RESEARCH FOR ADVANCED INERTIAL INSTRUMENTATION. TASK --ETC(U)
DEC 81 D DAS, K KUMAR, E WETTSTEIN, J WOLLAM N00014-77-C-0388
UNCLASSIFIED R-1528 NL

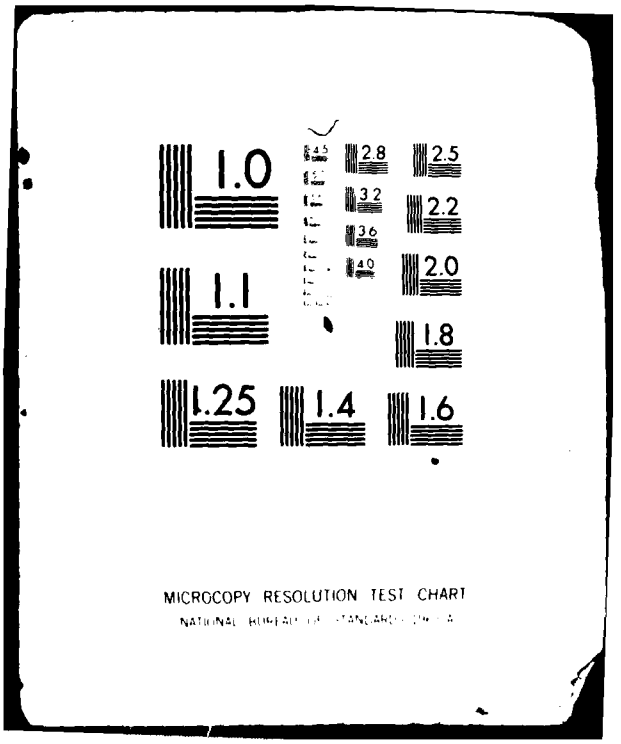
1.0
1.1
1.25
1.4
1.6
1.8
2.0
2.2
2.5
2.8
3.2
3.6
4.0
MICROCOPY RESOLUTION TEST CHART

SUPPLEMENTARY DISTRIBUTION LIST

Organization	Copies
Jack Bouchard Northrop/PPD 100 Morse Street Norwood, MA 02062	1
Howard Schulien Department 6209 Bendix Corporation Guidance Systems Division Teterboro, NJ 07608	1
Don Bates Honeywell, Inc. Aerospace Divison 11350 U.S. Highway 19 St. Petersburg, FL 33733	1
R. Baldwin Honeywell, Inc. Avionics Division 2600 Ridgway Parkway Minneapolis, MN 55413	1
Bus Brady 62-11B/1 Lockheed Missile and Space Co., Inc. P.O. Box 504 Sunnyvale, CA 94088	1
Dan Fromm MS 1A1 Delco Electronics 7929 South Howell Avenue Milwaukee, WI 53201	1
F. Mikoliet Autometics Division Rockwell International 3370 Miraloma Avenue Anaheim, CA 92803	1
P. Jacobson Sperry Flight Systems P.O. Box 21111 Pheonix, AZ	1
George R. Costello Senior Staff Engineer Control and Electromechanical Subdivision Guidance and Control Division The Aerospace Corporation P.O. Box 92957 El Segundo, CA 90009	1
John Hanks Dynamics Research Corp. 60 Concord Street Wilmington, MA 01887	1
D. Riley Systems Group, Minuteman TRW Inc. P.O. Box 1310 San Bernardino, CA 92402	1
Professor Robert Ogilvie Department of Materials Science and Engineering Massachusetts Institute of Technology Cambridge, MA 02139	
Dr. Glen R. Buell (D. Starks) AFML/MBT Wright-Patterson Air Force Base Dayton, OH 45433	1
Major George Raroha AFAL/CC Wright-Patterson Air Force Base Dayton, OH 45433	1

SUPPLEMENTARY DISTRIBUTION LIST (Continued)

Organization	Copies	Organization	Copies
Joe Jordan Litton Guidance and Control Systems 5500 Canoga Avenue Woodland Hills, CA 91364	1	Lt. Col. Gaylord Green Capt. Ken Wernle BMO/MNNG Norton Air Force Base San Bernardino, CA 92409	1
Bob Delaney Singer-Kearfott Division 150 Totowa Road Wayne, NJ 07470	1	Dave Gold (SP-230) Rick Wilson (SP-23411) Andy Weber (SP-23411) Strategic Systems Project Office Department of the Navy Washington, DC 20390	1
Elmer Whitcomb Sperry Gyroscope Division Great Neck, NY 11020	1	Lt. Col. Larry Fehrenbacker HQ/AFSC Andrews AFB, MD	1
C. Hoenig J. Holt R. Landingham Lawrence Livermore Laboratory University of California at Berkeley Livermore, CA 94550	1	N. Stuart (MMIRME) ALC/Ogden Ogden Air Logistics Command Hill AFB Ogden, UT 84404	1
Capt. S. Craig Aerospace Guidance Metrology Center Newark Af Station Newark, OH 43055	1	Professor R.M. Latanision Massachusetts Institute of Technology 77 Massachusetts Avenue Room E19-702 Cambridge, MA 02139	1
W. Lane Hamilton Standard Windsor Locks, CN	1	Dr. Jeff Perkins Naval Postgraduate School Monterey, CA 93940	1
Dr. A.G. Evans Department Material Sciences and Engineering University of California Berkeley, CA 94720	1	Dr. R.P. Wei Lehigh University Solid Mechanics Bethlehem, PA 18015	1
Professor H. Herman State University of New York Material Sciences Division Stony Brook, NY 11794	1	Professor H.G.F. Wilsdorf University of Virginia Department of Materials Science Charlottesville, VA 22903	

SUPPLEMENTARY DISTRIBUTION LIST (Continued)

Organization	Copies	Organization	Copies
Professor J.P. Hirth Ohio State University Metallurgical Engineering Columbus, OH 43210	1	Larry Pope Sandia National Laboratories Division 5833 Alburquerque, NM 81785	1
Professor Peter Gielisse University of Rhode Island Division of Engineering Research Kingston, RI 02881	1	Professor David Turnbull Harvard University Division of Engineering and Applied Physics Cambridge, MA 02139	1
Mr. R.W. Rice Code 6360 Naval Research Laboratory 4555 Overlook Avenue, S.W. Washington, DC 20375	1	Dr. D.P. H. Hasselman Montana Energy and MHD Research and Development Institute P.O. Box 3809 Butte, MT 59701	
Professor G.S. Ansell Rensselaer Polytechnic Institute Department of Metallurgical Engineering Troy, NY 12181		Dr. L. Hench University of Florida Ceramics Division Gainesville, FL 32601	1
Professor J.B. Cohen Northwestern University Department of Materials Sciences Evanston, IL 60201	1	Dr. J. Ritter University of Massachusetts Department of Mechanical Engineering Amherst, MA 01002	1
Professor M. Cohen Massachusetts Institute of Technology Department of Metallurgy Cambridge, MA 02139		Professor G. Sines University of California at Los Angeles Los Angeles, CA 90024	
Professor J.W. Morris, Jr. University of California College of Engineering Berkeley, CA 94720	1	Director Materials Sciences Defense Advanced Research Projects Agency 1400 Wilson Boulevard Arlington, VA 22209	1

SUPPLEMENTARY DISTRIBUTION LIST (Continued)

Organization	Copies	Organization	Copies
Professor O.D. Sherby Stanford University Materials Sciences Division Stanford, CA 94300	1	Professor H. Conrad University of Kentucky Materials Department Lexington, KY 40506	1
Dr. E.A. Starke, Jr. Georgia Institute of Technology School of Chemical Engineering Atlanta, GA 30332	1